

UNIVERSITY OF TARTU
FACULTY OF SCIENCE AND TECHNOLOGY
Institute of Chemistry

JAANUS LIIGAND

**ELECTROSPRAY IONISATION EFFICIENCY SCALES:
MOBILE PHASE EFFECTS AND TRANSFERABILITY**

Master's thesis (30 EAP)

Supervisor: Anneli Kruve, Ph D

Kaitmisele lubatud

Juhendaja

allkiri, kuupäev

Tartu 2015

Contents

Abbreviations	3
Introduction	4
1. Review of Literature.....	5
1.1 Electrospray Ionisation	5
1.1.1 Ionisation Efficiency	5
1.1.2 Solvent Effects on Electrospray Ionisation Efficiency	6
1.1.3 Physico-chemical Properties and Their Effect on Electrospray Ionisation Efficiency	8
1.1.4 Comparison of Studies on Different Mass Spectrometric Setups	10
2. Experimental.....	11
2.1 Reagents.....	11
2.2 Equipment.....	13
2.3 IE Measurement and Calculations	15
2.4 Independent Validation.....	17
3 Results.....	18
4 Discussion.....	27
4.1 Mobile Phase Effects	27
4.1.1 Comparison with Earlier Results.....	27
4.1.2 The Impact of Solvent pH	27
4.2 Ionisation Efficiency Scale Universality	30
4.2.1 Electrospray Source Design and Solution Properties.....	30
4.2.2 Mass Spectrometer Properties	31
4.3 Usefulness of Ionisation Efficiency Scales	31
4.4 Independent Validation.....	32
Conclusions	33
References	34
Kokkuvõtte	39
Acknowledgements	40
Appendix	41

Abbreviations

α	Ionisation degree
CE	Capillary electrophoresis
ESI	Electrospray ionisation
HOMO	Highest occupied molecular orbital
HPLC	High performance liquid chromatography
<i>IE</i>	Ionisation efficiency
LC	Liquid chromatography
$\log P$	Logarithm of partition coefficient
m/z	Mass to charge ratio
MS	Mass-spectrometry
pK_a	Negative logarithm of acidity constant
<i>TM</i>	Target mass

Introduction

Liquid chromatography electrospray ionisation mass spectrometry (LC/ESI/MS) is a very widely used analytical method. Most of the drug screening, food safety and environmental analyses are done with LC/ESI/MS. Although the ESI interface is commercially available since the beginning of the 90s the mechanism of ESI is not fully understood.

It is known that at equal concentrations give different signals in mass spectrometer. Therefore standard compounds are needed to estimate the concentration of the analytes. In many applications (*e.g.* metabolomic studies and pollutant screening) the standard compounds are rarely if at all available. In such cases a standard substance free quantification model would be very helpful.

One possibility to solve this problem is via ionisation efficiency scales. If one is capable of accurately predicting compounds' ionisation efficiencies the standard substance free quantification would become available for everyone.

In literature there are some studies about analyte properties that affect ionisation efficiency. Unfortunately little attention is paid to the quantitative study of mobile phase effects on ionisation efficiency. Additionally, the obtained results are not always consistent, raising the question if conclusions made on one instrument are transferable to another. This study will fulfil this gap.

The aim of this thesis therefore is:

- to study the effect of solvent pH on electrospray ionisation efficiencies,
- to study the effect of organic solvent content on ionisation efficiencies and
- to study the effects of instrument type on ionisation efficiencies.

To fulfil these aims, 14 ionisation efficiency scales were established in ESI positive ion mode, covering altogether 4 instruments, 7 solvent systems and 97 solvent-compound combinations.

1. Review of Literature

1.1 Electrospray Ionisation

Electrospray ionisation mass spectrometry (ESI/MS) is a widely used method to determine biomolecules (used in metabolomics, proteomics, lipidomics etc), pesticides, pollutants and doping substances [1]. Electrospray ionisation can be coupled with separation techniques such as high performance liquid chromatography (HPLC) and capillary electrophoresis (CE) [2].

In 1984 John B. Fenn and Masamichi Yamashita introduced the electrospray approach connected to mass spectrometry [3, 4]. The significance of ESI/MS was recognised with a Nobel Prize in 2002 to John B. Fenn, who was the major developer of the method [5].

There are three major steps in the electrospray process. These are: a) production of charged droplets at the ESI capillary tip; b) shrinkage of charged droplets by solvent evaporation and repeated droplet fission leading to very small highly charged droplets capable of producing gas phase ions; and c) producing the gas phase ions from these droplets [1].

Both positive and negative ionisation can be used with ESI [2, 6-11]; the positive ionisation is remarkably more popular. In this work only the positive ion mode is studied.

1.1.1 Ionisation Efficiency

Although ESI/MS is widely used, the mechanism is still fuzzy and the majority of users apply it as a “black box”.

It is known that responses obtained with different analytes differ remarkably [7,8,10,12-18]. Those differences arise from the fact that depending on the analyte a different amount of gas phase ions can be generated from the same amount of molecules in the liquid phase. This effect is called the ionisation efficiency. Till one does not understand the mechanism of ionisation, standards are needed for quantitative analysis. There is a lack of standard substances for many applications (e.g. metabolomics). Therefore, it would be very useful to predict the ionisation efficiencies from physico-chemical properties of analytes and eluent. Models predicting ionisation efficiencies can be built only if reliable quantitative data of ionisation efficiencies are available. One possibility for collecting such data is via ionisation efficiency scales. Ionisation efficiencies have been studied for both positive [7,8,10,12,13,16,19,20] and negative modes [15,18,21].

A number of aspects are known to affect the ionisation efficiency. Firstly, the analyte has to be charged. In the positive ionisation the ions are either intrinsically charged [22], formed by

protonation [7,17,20] or adduct formation with cations such as sodium [17], ammonium [23,24] or formed by electrochemical oxidation in the electrospray needle [25].

Secondly, the ion has to desorb from the droplet to gas phase. There are two main models describing how the ions enter the gas phase: the charge residue model [23] and the ion evaporation model [24]. Kebarle and Peschke [26] have shown that the ionisation of small molecules is described better with the ion evaporation model. According to Iribarne's ion evaporation theory, ions enter the gas phase when solvent evaporation increases the charge density on the droplets to the extent that Coulombic repulsion overcomes the analyte solvation interactions [24]. This causes the ions to "evaporate" from the droplet surfaces [24]. In this study more attention is paid on small molecules and thus it is assumed that ionisation occurs via the ion evaporation model.

1.1.2 Solvent Effects on Electrospray Ionisation Efficiency

The ionisation efficiency does not depend only on the analyte itself. The different solvent systems can enhance or decrease the ionisation efficiency [18,22,27-29]. Instrument parameters affect ionisation efficiency as well [30].

The ESI process starts with charge separation that is achieved with a strong electric field at the ESI emitter tip. The conductivity of the solvent has to be sufficient for efficient charge separation if high sensitivity and good spray-stability are desired. Solvents suitable for ESI vary from solvents with high polarity to medium polarity. Water, methanol and acetonitrile are mostly used [27]. Water alone is a poorer solvent than pure methanol, acetonitrile or dichloromethane [31].

Once the initial charged droplets have been formed, the efficiency to emit gas phase ions is dependent on the surface tension and volatility of the solvent [6]. The relatively poor sensitivity for analytes dissolved in water has been attributed to higher surface tension, low volatility and efficient solvation of ions in water [31]. These effects are proved with molecular dynamics simulations as well [32].

Nowadays the most used solvents are mixtures of organic modifier and buffer solution and the ESI sources are typically pneumatically assisted. Thus the high surface tension and low volatility do not affect the ESI efficiency so drastically. At the same time it is possible to modify ESI signal remarkably by choosing proper conditions [18].

Iribarne et al. [24] suggested that there is a crossing point in droplet radius when Coulomb fission is taken over by ion evaporation. Therefore when the droplet radius decreases quicker,

the crossing point is achieved earlier and the ions have more time to evaporate, resulting in higher ionisation efficiency. The organic phase percentage affects the droplet “drying” rate. Girod et al. [30] have shown that higher organic phase content results in quicker decrease of droplet radius. Ahadi and Konermann [32] also confirmed this effect with molecular dynamics simulations. Zhou and Hamburger [33] have shown that the higher the organic phase content in the solvent is, the higher the ionisation efficiency will be. In some cases, however, organic content above 80% can actually result in decreased ESI response [33]. Lower organic phase percentage results in higher surface tension, which delays reaching Rayleigh limit and ions have less time to evaporate [28].

It has also been observed by Girod et al. [30] that the droplet’s organic modifier content changes remarkably during electrospray. Initial higher organic phase content results in higher fractionation.

Additionally, Ahadi and Konermann [32] have shown that for mobile phases with low (~25%) organic phase content partition of organic solvent molecules and water molecules between droplet periphery and interior occurs. They also showed with molecular dynamics simulations that higher organic phase percentage results in higher amount of ejected ions. In previous studies Ahadi and Konermann showed that the excess charge is situated on the 2/3 of droplet radius in case of Na⁺ [34] as well as in case of H⁺ [35]. In addition, Ahadi and Konermann [32] have explained the ion-evaporation process. The droplet surface is undulating and the ion with solvent cluster is ejected from tip of surface protrusions. Solvent bridging prior to ion ejection is more extensive for methanol/water droplets than for purely aqueous systems [32].

Often the higher sensitivity in ESI is achieved when the analyte is ionised already in a liquid phase. Therefore in case of basic analytes the acidic mobile phase is preferred [27]. However, Mallet et al. [36] have shown that higher used acid concentrations result in drastically decreased intensities. Zhou and Cook [37] have shown that “wrong-way-round ionisation” also exists. For example, high sensitivity in positive ion mode is achieved for basic compounds by using a basic mobile phase containing ammonia [27]. One explanation for this phenomenon could be gas phase proton transfer reaction. The gas-phase proton transfer reaction is dependent on the amount of reagent ions in the gas phase. Mallet et al. [36] have shown that increasing the ammonia concentration from 0.05% to 1% also increases the ESI response of basic analytes in positive mode up to two times. Controversially, in case of ion evaporation model the higher additive concentration could result in decreased ESI response [19].

Girod et al. [38] have additionally shown that solvent pH changes remarkably during the ESI process. In negative ion mode the pH decreases along the plume if initial pH < 7 and increases if pH > 7. In positive ion mode the pH at tip exit is higher than pre-sprayed pH value due to electrochemical processes on the needle wall [39]. If the solution with initial pH 7.0 is sprayed in negative and positive ion mode the pH increases in case of negative ion mode and inversely decreasing in case of positive ion mode [38].

Typically, the water phase pH is meant while discussing solvent pH. Additionally, one should consider that organic solvent affects the solvent pH. For example, increasing acetonitrile percentage results in higher pH value for acidic buffers [29]. Additionally, the organic phase affects the acidity constant (pK_a) of an analyte. For example the pK_a of acetic acid increases two units and the pK_a of amines decreases one unit between water and acetonitrile/ water 40:60 (v/v) [29,40].

Amad et al. [19] studied the gas phase basicities of used solvents and analytes and found that solvents with higher proton affinities in the gas phase suppress the ionisation of analytes.

Tang and Kebarle [11] and Cech and Enke [12] have shown that high concentrations (analytes or overall electrolytes) suppress the analyte's signal. Tang and Kebarle [11] proposed an equation to calculate the MS signal for compound A:

$$I_{A^+} = Pf \cdot \frac{k_A [A^+]}{k_A [A^+] + k_E [E^+]}, \quad \text{I}$$

where P is the sampling efficiency of the mass spectrometer and f is the fraction of the charge on the droplet leaving the needle that is converted to gas-phase ions, $[E^+]$ denotes the net concentration of all electrolyte ions present in the electrosprayed solution, and k_A and k_E express the relative efficiency with which A and E is converted into gas phase ions.

1.1.3 Physico-chemical Properties and Their Effect on Electrospray Ionisation Efficiency

Scientists investigating ESI have been trying to find out which molecular parameters influence ionisation efficiency. For example, in positive ion mode ionisation via protonation has been correlated with: pK_a [15,16], partition coefficient ($\log P$) [7], molecular volume [7,16], absolute mobility [7], adjusted molecular mass ($H/C \cdot \text{molecular mass}$) [41] and effective charge [7]. Results of Ehrmann et al. [8] have shown that gas phase basicity does not show significant correlation with ionisation efficiency, but the pK_b of analytes in solution does affect ionisation efficiency.

Also, some predictions of ionisation efficiency based on other physico-chemical parameters have been proposed in the literature. Chalcraft et al. [7] modelled the ionisation efficiency based on molecular volume, octanol-water distribution coefficient, absolute mobility and effective charge. The predicted ionisation efficiencies were statistically significantly correlated with molecular volumes and octanol-water distribution coefficients. The model was based on different metabolites – amino acids and their derivatives. Although the model gives quite accurate results (R^2 was 0.83 and intermediate error was 40%), the test compounds were all very hydrophilic compounds, the ionisation efficiency scale covered only one $\log IE$ unit and it has been tested only for one solvent composition.

Oss et al. [16] have established a large ESI ionisation scale of compounds with various properties. The ionisation efficiencies were correlated with different molecular properties and significant correlation was observed with molecular volume and basicity of the molecules. Although the model covers 6 $\log IE$ units and gives satisfactory accuracy, the model does not account for solvent effects.

Nguyen et al. [41] found that ESI sensitivity in positive mode is positively correlated with the adjusted molecular mass ($H/C \cdot \text{molecular mass}$). However, in this study only a single solvent composition was used and the model was established based on four analytes.

In negative ion mode there are also some studies that correlated responses with different molecular parameters: pK_a [15,18,21], $\log P$ [18,21], charge delocalisation degree [21]. Henriksen et al. [15] studied negative ionisation and their results showed that ionisation efficiency dependence on pK_a is more complex and the hydrophobicity ($\log P$) of a compound affects its ionisation efficiency remarkably. Huffman et al. [18] extended the Henriksen et al. [15] study (neat methanol and acetonitrile and 1:1 mixture of acetonitrile and water and methanol and water) with solvents (neat water and acetone combinations) and with analytes that have a wider span of pK_a and $\log P$ values. They found that in general the ionisation efficiency increases if in the homological compound set the alkyl chain length increases and specifically, in the family of phenols introducing electron acceptor substituent increases the ionisation efficiency. The results also showed that in negative ionisation the protic polar solvent increases the ionisation efficiency [18].

Krube et al. [21] studied negative ion mode and developed a prediction model based on WAPS (charge delocalisation in the anion) and degree of ionisation. Although the model is developed using a scale covering more than 4 $\log IE$ units and taking into account the solvent pH, it is established in one solvent only.

Wu et al. [42] modelled the ionisation efficiency based on computational descriptors. Statistically significant descriptors were hydrogen bond acidity, highest occupied molecular orbital (HOMO) energy, the number of hydrogen bond donating groups, the ratio of organic phase and polar solvent accessible surface. Although the proposed model shows quite good accuracy, it is based on narrow distribution of compounds.

Unfortunately, most of the proposed models neither in positive nor in negative ion mode do not take solvent properties into account. Also, since these models proposed by different groups are somewhat different it also raises the question if a model proposed on one instrument is applicable on another instrument.

1.1.4 Comparison of Studies on Different Mass Spectrometric Setups

The mostly used mass analysers for electrospray ionisation mechanism studies are ion-trap [7,8,16,20,21] and triple quadrupole [15,18,19,42]. Only in few cases direct comparison of the obtained results is possible, because in most cases the studied compounds and solvent systems differ. As an example, mutually consistent results were observed by Henriksen et al. [15] and Huffman et al. [18] although they used different ESI source designs (without and with sheath gas), different applied voltages (-2.8 kV and -1.5 kV), and different drying gas temperatures (250 °C and 350 °C). The analytes that were found to be good responders by Henriksen et al. [15] also gave good response in the study by Huffman et al. [18]. However, numerical comparisons of ionisation efficiencies for different instruments cannot be made based on the published data.

Although the scale of ref. [16] has been used a lot, there have been no attempts to reproduce even a subset of the measurements on a different MS system with different ion source. The only work known, that offers at least some possibility of comparing results is that of Ehrmann et al. [8]. The responses obtained in ref. [8] show good consistency with results presented in ref. [16] except for diphenylamine, which has good response in ref. [16] scale but showed weak response in ref. [8] study. Both studies used ion trap mass spectrometer but different ESI setups (nanoESI [8] and ESI with assisted nebulisation [16]), applied voltages (1.5 kV and 3.5 kV), temperatures (150 °C and 350 °C) and solvents (99.5% methanol and 0.5% acetic acid in one case, and 80% (v/v) acetonitrile and 20% of ultra-pure water with 0.1% formic acid in the other studies) were used. Thus, although rather voluminous ESI IE scales exist for negative and positive ion modes, their validity on different MS systems with different ESI sources has not been demonstrated. Therefore, the validity of prediction models on different instrumental setups has also not been demonstrated either.

2. Experimental

2.1 Reagents

The compounds included in the establishment of the ionisation efficiency scales were diphenyl phthalate (Assay 99.9% by GC, Riedel-de Haën), dimethyl phthalate (Assay $\geq 99\%$ by GC, Merck), tetrapropylammonium chloride (purum; $\geq 98.0\%$ (AT), Fluka Analytical), tetraethylammonium perchlorate (puriss., Fluka), N,N-dimethylaniline (pure, Reakhim), 1-naphthylamine (pure, Reakhim), piperidine ($>99.5\%$, Sigma-Aldrich), pyrrolidine ($>98\%$, Fluka), pyridine ($>99.8\%$, Fluka), triethylamine (99%, Aldrich).

Tetramethylammonium chloride (puriss. p.a., for ion pair chromatography, Fluka Analytical), 2-nitroaniline (pure for analysis), benzamide (pure Reakhim), 2,6-dimethylpyridine (pure for analysis), DBU (pure for analysis, see structure in Table S 1), acridine ($>97\%$, Fluka), tetrabutylammonium perchlorate ($\geq 99.0\%$, Fluka), tetrahexylammonium benzoate (Kodak), diphenylguanidine (pure Reakhim), pyridine ($>99.8\%$, Fluka), triethylamine (99%, Aldrich), piperidine ($>99.5\%$, Sigma-Aldrich), N,N-dimethylaniline (pure, Reakhim), tetraethylammonium perchlorate (Fluka, puriss.), tetrapropylammonium chloride (Fluka Analytical, purum; $\geq 98.0\%$ (AT)) were used in the validation experiments (see 2.4).

For water phase pH effects study additionally following compounds were analysed: 3-methoxy-N,N-dimethylaniline (purified using crystallisation from ethanol, Sigma-Aldrich), 2,4-dinitroaniline (98%, Sigma-Aldrich), 3-nitroaniline (98%, Sigma), 4-nitroaniline ($\geq 99\%$, Sigma), dimethylphenylphosphine (99%, Aldrich), trimethylphosphine (97%, Aldrich), 4-aminobenzoic acid ($\geq 99\%$, Sigma), quinoline ($\geq 99\%$, Aldrich), 2-aminophenol (99%, Aldrich), 3-aminobenzoic acid ($\geq 99.0\%$, Fluka), 2,6-diaminopyridine (99+%, Aldrich), 8-aminoquinoline (pure, Reakhim), 2-aminobenzimidazole ($>97\%$, Aldrich), N,N-diphenylbispidine [44], 2,4,6-trinitroaniline ($\geq 99\%$, Sigma), 2-aminopyridine ($\geq 99\%$, Aldrich), 4-(dimethylamino)-N,N-dimethylaniline (purified using crystallisation from ethanol, Merck), trizma® base ($\geq 99.9\%$, Sigma), 4-amino-N,N-dimethylaniline (purified using crystallisation from ethanol, Sigma), 3-hydroxypyridine (98%, Aldrich), 3-(dimethylamino)benzoic acid ($\geq 97\%$, Sigma), tetramethylammonium chloride (puriss. p.a., for ion pair chromatography, Fluka Analytical), 2-nitroaniline (98%, Aldrich), tetraethylammonium perchlorate (puriss, Fluka), aniline (puriss p.a, Sigma-Aldrich), 2,6-dimethylpyridine (pure for analysis, Reakhim), 1-naphthylamine (pure, Reakhim), pyridine ($>99.8\%$, Fluka), N,N-dimethylaniline (pure, Reakhim), acridine ($>97\%$, Fluka). 2,6-(NO₂)₂-C₆H₃-P1(pyrr) phosphazene (see structure Table S 1, [43]).

The compounds included in the target mass (either providing $[M+H]^+$, $[M+Na]^+$ or fragments) study were (mass to charge ratio (m/z) value refers to the ion formed in the ESI source): ethylamine hydrochloride ($m/z = 46$, 98%, Aldrich), guanidine ($m/z = 60$, pure, Reakhim), pyrrolidine ($m/z = 72$, >98%, Fluka), tetramethylammonium chloride ($m/z = 74$, puriss. p.a., for ion pair chromatography, Fluka Analytical), pyridine ($m/z = 80$, >99,8%, Fluka) piperidine ($m/z = 86$, >99.5%, Sigma-Aldrich), aniline ($m/z = 94$, puriss p.a, Sigma-Aldrich), triethylamine ($m/z = 102$, 99%, Aldrich), 1-ethyl-3-methylimidazolium trifluoromethanesulfonate ($m/z = 111$, high purity, Merck), 1,1,3,3-tetramethylguanidine ($m/z = 116$, 99%, Aldrich), N,N-dimethylaniline ($m/z = 122$, pure, Reakhim), tetraethylammonium perchlorate ($m/z = 130$, puriss., Fluka), 4-nitroaniline ($m/z = 139$, pure for analysis), 1-naphtylamine ($m/z = 144$, pure, Reakhim), 4-fluoro-3-nitroaniline ($m/z = 157$, 97%, Sigma-Aldrich), dimethyl glutarate ($m/z = 161$, $\geq 99\%$ by GC, Merck), 1-hexyl-3-methylimidazolium bis(trifluoromethanesulfonyl)imide ($m/z = 167$, high purity, Merck), sulfanilamide ($m/z = 173$, for microanalysis, Carlo Erba), acridine ($m/z = 180$, $\geq 97\%$ (HPLC), Fluka), tetrapropylammonium chloride ($m/z = 186$, purum; $\geq 98.0\%$ (AT), Fluka Analytical), aldicarb ($m/z = 191$, analytical standard, Dr. Ehrenstorfer), dimethyl phthalate ($m/z = 195$, $\geq 99\%$ by GC, Merck), imazalil ($m/z = 201$; 255; 297, analytical standard, Dr. Ehrenstorfer), diphenylguanidine ($m/z = 212$, pure, Reakhim), oxamyl ($m/z = 220$; 242, analytical standard, Dr. Ehrenstorfer), methiocarb ($m/z = 226$, analytical standard, Dr. Ehrenstorfer), triphenylamine ($m/z = 246$, pure, recrystallised once from ethanol (96%), Reakhim), $((CH_3)_2N)_3-P=N-C_6H_5$ ($m/z = 255$, [43]), imidacloprid ($m/z = 256$; 278, analytical standard, Dr. Ehrenstorfer), vamidothion ($m/z = 288$, 310, 99.0%, Dr Ehrenstorfer GmbH), buprofezin ($m/z = 306$, analytical standard, Dr. Ehrenstorfer), epoxiconazole ($m/z = 330$, analytical standard, Dr. Ehrenstorfer), fluquinconazole ($m/z = 376$, analytical standard, Dr. Ehrenstorfer), 2,6-(NO₂)₂-C₆H₃-P1(pyrr) ($m/z = 423$, [43]), 2,6-Cl₂-4-NO₂-C₆H₂-P1(pyrr) phosphazene ($m/z = 447$, [43]), N,N'-(CHPh₂)₂-bispidine ($m/z = 459$, [44]), 9-O-1,5-N,N'-(CHPh₂)₂-bispidine ($m/z = 473$, [44]), EtP2(dma) ($m/z = 494$, Sigma Aldrich >98%), PhP2(pyrr) ($m/z = 518$, [43]) and (C₄H₈N)₃-P=N-(C₄H₉N)₂-P=N-C₆H₄-2-Cl ($m/z = 552$, [43]).

Acetonitrile (J. T. Baker, Deventer, The Netherlands, HPLC grade and Chromasolv® gradient grade Plus for HPLC, $\geq 99.9\%$ Sigma-Aldrich, USA), ultra-pure water (purified with Millipore Advantage A10 MILLIPORE GmbH, Molsheim, France), formic acid (Fluka, 98%), trifluoro acetic acid (99+%, Aldrich), ammonia solution (25%, Lach:Ner) and ammonium acetate ($\geq 99.0\%$ Fluka) were used as solvent components.

Seven different mobile phase compositions were studied: three different acetonitrile percentages 20%, 50% and 80% and different water phases with pH 2.7, 5.0 and 9.7. pH = 2.7 was obtained with 0.1% formic acid and pH=9.7 with 1mM ammonia. Buffer with pH 5 was obtained with adjusting the pH of 5 mM ammonium acetate solution with formic acid.

The studied solvent compositions were:

- (1) 80% (v/v) of acetonitrile and 20% of 0.1% formic acid in ultra-pure water,
- (2) 50% (v/v) of acetonitrile and 50% of 0.1% formic acid,
- (3) 20% (v/v) of acetonitrile and 80% of 0.1% formic acid,
- (4) 80% (v/v) of acetonitrile and 20% of ammonium acetate buffer pH=5.0,
- (5) 50% (v/v) of acetonitrile and 50% of ammonium acetate buffer pH=5.0,
- (6) 80% (v/v) of acetonitrile and 20% of 1mM ammonia, and
- (7) 50% (v/v) of acetonitrile and 50% of 1mM ammonia.

Additionally two mobile phases acetonitrile/0.1% trifluoro acetic acid (pH=2.1) 80:20 (v/v) and acetonitrile/pH=7.0 buffer (5mM ammonium acetate adjusted with ammonia) 80:20 (v/v) were used to study pH effects further.

2.2 Equipment

The ionisation efficiency measurements were carried out, in the positive ion mode, on three different mass-spectrometers. The first instrument was an Agilent XCT ion trap mass spectrometer (Agilent Technologies, Santa Clara, CA, USA). For instrument control Agilent ChemStation for LC Rev. A. 10.02 and MSD Trap Control Version 5.2 were used. Two types of ESI sprayers were used: conventional (see Figure S 1) and in-house developed 3R sprayer [45] (see Figure S 4). MS and ESI parameters used for the conventional sprayer were: nebuliser gas pressure 15 psi, drying gas flow rate 7 L/min, drying gas temperature 300 °C, additionally only target mass (*TM*) was optimised. For 3R sprayer [45] nebuliser gas pressure was 2 psi, drying gas flow rate 10 L/min, drying gas temperature 350 °C, and inner capillary gas pressure 12 bar. For both setups the needle voltage was 3500 V.

The second mass spectrometer was a Varian J-320 (Varian Inc., Walnut Creek, CA, USA) triple quadrupole mass spectrometer. For the instrument control, MS Workstation 6.9.2 was used. ESI source with an angular geometry was used (see Figure S 2). Nebulisation parameters were: needle voltage 3500 V, drying gas 10 psi, drying gas temperature 300 °C, and shield voltage

300 V. The signal was recorded with capillary voltages 30 V, 40 V, 50 V, 60 V, 70 V. The highest obtained signal was used.

The third mass spectrometer was a single quadrupole mass spectrometer Single Quad 6100 equipped with the modified [30] Agilent Jet Stream (AJS) ESI Source (Agilent Technologies, Santa Clara, CA, USA; (see Figure S 3). Used ESI parameters were: capillary voltage 3500 V, nozzle voltage 600 V, nebuliser gas pressure 15 psi, drying gas flow rate 7 L/min, drying gas temperature 300 °C, sheath gas flow rate 1 L/min and sheath gas temperature 80 °C. The same instrument with the same setup was also used for solvent fractionation measurements.

For independent validation study Varian 910-FT-ICR-MS system was used. Solutions were infused into a mass spectrometer with a flow rate of 0.5 mL/h. For the instrument control, MS Workstation 6.9.2 and Omega 9.2.29 were used. The used ESI source has an angular geometry (see Figure S 2) and the nebulisation parameters used were: needle voltage 3500 V, drying gas pressure 10 psi, drying gas temperature 300 °C, shield voltage 300 V and capillary voltage 30 V.

For solvent fractionation measurements the optical spray plume profiling setup was coupled with the mass-spectrometer via the Agilent Jet Stream ESI Source. The fluorescence equipment is described in details in ref. [38]. Briefly, it consists of an excitation laser and an optical detection system mounted on a moving stage. A continuous wave laser ($\lambda = 532$ nm) emitting in a single longitudinal mode was used to profile the ESI plume. The output power of the laser was 300 mW and its beam diameter was 0.3 mm (divergence 1.2 mrad). The laser beam was focused into the spray and the fluorescence was collected by an objective used in an epifluorescence configuration. Fluorescence spectra of fluorescent dyes from the ESI plume were recorded, point by point (pixel size 500 μm), by an ultra-compact spectrophotometer.

Nile Red was used as a solvatochromic (polarity-sensitive) fluorescent dye for profiling the solvent composition in the ESI plume. The solvatochromism of Nile Red is due to differences in fluorescence spectra according to the polarity of the solvent. First of all, the chromism of this dye was calibrated in different acetonitrile/water binary solvent mixtures with 1 mM ammonia. As the fraction of water in the mixed solvents increases, the wavelength of maximum emission λ_{max} shifts to longer wavelength. The solvent composition of an unknown solution can be determined based on λ_{max} using a linear calibration graph. Because the ESI source produces charged droplets with relatively high temperature, it is shown that the spectroscopic properties of Nile Red were not significantly affected by these parameters [30]. The different

concentrations of Nile Red in the ESI plume, due to changes in droplet size, will have an influence on the fluorescence intensity, but as we used the maximum emission λ_{\max} (which remains constant with the concentration) for estimation the calibration curve is valid.

The aqueous phase pH was measured with pH-meter (Evikon pH Meter E6115) using glass electrode (Evikon pH631).

2.3 IE Measurement and Calculations

All *IE* measurements were carried out using optimised *target mass* (TM) values for each ion. The compounds' solutions were mixed together by the t-piece so that the overall solution flow rate was 0.5 mL/h (concentrations of the studied compounds in spray were in the range of $5 \cdot 10^{-7}$ to $4 \cdot 10^{-5}$ mol/L).

In calculations only the signals of the molecular ion (either M^+ or $[M+H]^+$) and fragmentation products of the protonated species were taken into account. The ionisation efficiency has been defined earlier [14] as:

$$IE(M_i) = \frac{R_i}{C_i}, \quad \text{II}$$

where R_i is the MS response of the ion $[M+H]^+$ (plus possible fragments formed from it) at concentration C_i . As it is complicated to measure absolute ionisation efficiencies measuring the *Relative Ionisation Efficiency* (*RIE*) of a compound M_1 relative to M_2 is preferred:

$$RIE(M_1, M_2) = \frac{IE(M_1)}{IE(M_2)} = \frac{C_2 R_1}{C_1 R_2}. \quad \text{III}$$

Logarithmic scale was used for better visualisation of the results. For one measurement five different concentration ratios of two analytes were measured and $\log RIE$ values were averaged.

The *IE* values were assigned to the compounds on the scales by a two-stage procedure.

As a first stage the individual ionisation efficiency scales were compiled using the same approach as in ref. [46], i.e. the $\log IE$ values were assigned to the compounds in such a way as to minimise the sum of squared differences *SS* between the differences of the directly measured $\log RIE(M_i, M_j)$ values and the assigned $\log IE(M_i)$ and $\log IE(M_j)$ values according to eq. IV. Tetrapropylammonium was used as temporary reference compound (M_i) in this stage.

$$SS = \sum_{k=1}^n \left\{ \log RIE_k(M_i, M_j) - \log IE(M_i) - \log IE(M_j) \right\}^2 \rightarrow \min, \quad \text{IV}$$

The overall number of measurements is denoted by n and $\log RIE_k(M_i, M_j)$ is the result of k -th measurement that has been conducted between compounds M_i and M_j .

As the second stage the obtained $\log RIE$ scales were anchored to literature $\log IE$ values of the compounds from ref. [16] using least squares minimisation according to eq. V. This stage essentially “shifts” the scales (while keeping their spans and the differences of the $\log IE$ values within the scales intact) with respect to each other and takes the measurements of all compounds into account, rather than arbitrarily selecting a single reference compound.

The final $\log IE$ values that form the characteristic scale on the corresponding mass spectrometer were obtained by minimising the squares of $\log IE$ values differences on different mass spectrometers according to equation V:

$$SS_2 = \sum_{i=1}^n [\log IE_1(B_i) - \log IE_2(B_i)]^2 \rightarrow \min, \quad \text{V}$$

where $\log IE_1(B_i)$ is the $\log IE$ value of base B_i obtained by absolute anchoring under the studied conditions on ion trap mass spectrometer and $\log IE_2(B_i)$ is $\log IE$ value of base B_i under the same conditions on a different mass spectrometer.

Unlike the transferability study the mobile phase study used only the first stage and additionally anchoring between different solvents.

In order to assign $\log IE$ values to analytes the scale in solvent composition (1) was anchored to tetrapropylammonium $\log IE$ value from ref. [16]. To anchor the scales of other solvent compositions the MS signal intensities of $4 \cdot 10^{-6}$ M tetrapropylammonium in all solvent compositions were measured on the same day and the $\log IE$ value of tetrapropylammonium in a solvent S_i was calculated using equation VI:

$$\log IE(S_i) = \log \left(IE(S_1) \cdot \frac{Signal(S_i) \cdot C(S_1)}{C(S_i) \cdot Signal(S_1)} \right), \quad \text{VI}$$

where $Signal(S_i)$ and $Signal(S_1)$ are the average tetrapropylammonium signal intensities in solvent composition i and 1 days and $C(S_1)$ and $C(S_i)$ are the tetrapropylammonium concentrations in the respective solvents.

The combined standard deviation of the ionisation efficiencies of the compounds on the scales was calculated using equation VII:

$$s_c = \sqrt{s_{consistency}^2 + s_{anchoring}^2}, \quad \text{VII}$$

where $s_{consistency}$ is the consistency standard deviation of scale and $s_{anchoring}$ is the arithmetic mean standard deviation of anchoring.

The ionisation degree of analytes in aqueous solution (α) was calculated using equation VIII:

$$\alpha = \frac{\text{protonated form}}{\text{sum of all forms}} = \frac{[H^+]}{[H^+] + K_a}, \quad \text{VIII}$$

where $[H^+]$ is hydrogen ion concentration in the aqueous phase and K_a is acidity constant of the protonated base (conjugate acid of the base) in water. Aqueous pH and pK_a values were used because (1) at the time of ion ejection the droplet in the case of all solvent compositions is predominantly composed of water (see Figure 2) (2) the ionised analyte is preferentially solvated by water molecules. It is important to note, though, that $[H^+]$ in droplet may differ significantly from bulk solution.

2.4 Independent Validation

For independent validation of ionisation efficiency scale inter-instrument transferability, a mixture of fifteen analytes in acetonitrile/0.1% HCOOH in pure-water 80/20 (v/v) solvent mixture was infused. The pH independent compounds – tetrahexylammonium, tetraethylammonium and tetramethylammonium – were chosen as calibrants. A correlation line between calibrants $\log IE$ values from ref. [16] and logarithm of sensitivity (signal to concentration ratio) was established. The obtained slope and intercept values were used to predict the concentration c_{calc} for each analyte according to equation IX:

$$c_{calc} = \frac{S}{10^{\log IE \cdot \text{slope} + \text{intercept}}}, \quad \text{IX}$$

where S is the signal from mass spectra, $\log IE$ is the tabulated ionisation efficiency from ref. [16] and slope and intercept are obtained from the correlation line.

All the statistical tests were carried out at 95% confidence level.

3 Results

For the first step in the ionisation efficiency study the target mass (TM) parameter was optimised. The target mass is an ion optics parameter of the MS system of Agilent XCT ion trap mass spectrometer that modifies ion transport efficiency in the MS. For TM optimisation analytes with m/z from 46 to 522 were measured at different TM values (from 15-1000 with increment of 10 units). At each TM value MS signal was recorded and averaged over 1.5 min. For each compound included in the study all of the MS responses were normalised against the highest intensity observed over all TM values.

The normalised signals with different TM values are present in Figure 1. The optimised TM values for ion trap mass spectrometer were following: the highest (at least 90% of maximum signal) signal for ions with $m/z < 180$ was obtained with $TM = 15$. Ions with the $m/z > 180$ showed a curved relation between m/z and TM . Different functions (linear, exponential, logarithmic and power) were fitted to the curve and the best fit was obtained with logarithmic function. So the optimal target mass was obtained by the equation X:

$$TM = 497 \cdot \ln(m/z) - 2317 \quad X$$

Therefore $TM = 15$ was used for most of analytes. Diphenylphthalate and dimethylphthalate fragment in source and the signals were obtained as the sum of molecular ions and fragments intensities at TM value optimal for corresponding ion.

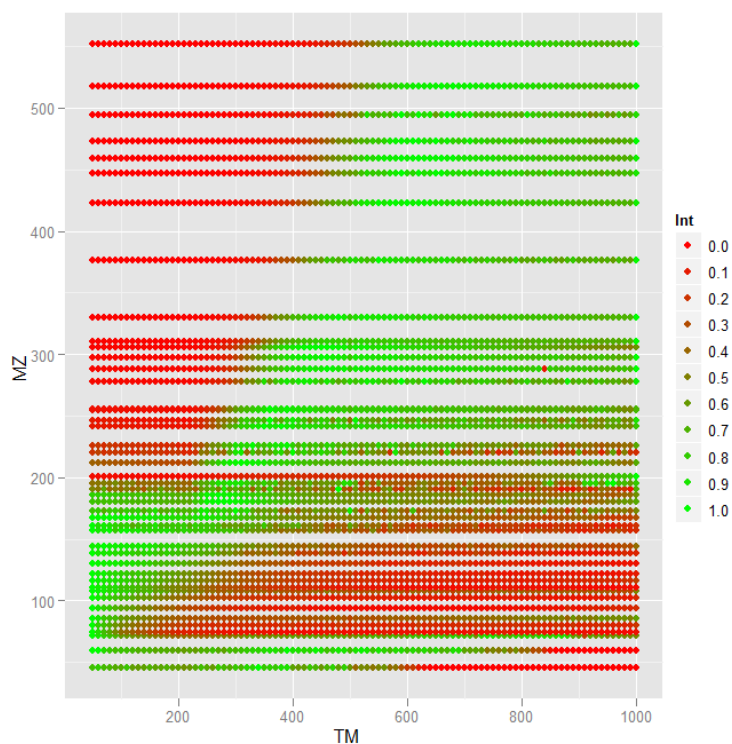


Figure 1. The relative intensities for peaks with m/z values ranging between 46 and 552 for target mass values between 50 and 1000 with increment of 10 m/z units. The colour of the dot indicates intensity relative (according to the scale brought on the right hand side) to the highest intensity observed for corresponding m/z : red dots indicate low intensity, green dots indicate high sensitivity.

The results of $\log IE$ measurements at optimal TM values and comparison with previous study (ref. [16]), that did not use thoroughly optimized TM values, are presented in Table 1. No statistically significant differences were observed.

Altogether 120 relative measurements with the 10 compounds (different extent of protonation (ionisation) in the solvent and different surface activity (hydrophobicity)) were carried out during 7 months in 7 solvent systems (three different acetonitrile percentages (20, 50, 80%) and three different water phases (pH=2.7, 5.0, 9.7)). In each solvent system an ionisation efficiency scale was constructed. The results are presented in Table 1. The widest of the resulting scales has a span around 5 orders of magnitude. In Table 2 t-test results of ionisation efficiency scales between different solvent systems are presented. The largest ionisation efficiency change with pH (from pH=2.7 to pH=9.7) was observed for pyridine (3.35 logarithmic units) and the largest $\log IE$ decrease with acetonitrile percentage decrease from 80% to 20% was 0.87 logarithmic units for pyrrolidine.

Table 1. The positive mode ESI ionisation efficiency ($\log IE$) values and the approximate ionisation degrees (α) in solution at different solvent compositions.

	Acetonitrile/ 0.1% HCOOH	Acetonitrile/ 0.1% HCOOH						Acetonitrile/ pH=5.0				Acetonitrile/ 1mM NH ₃			
	80/20 ^c	80/20 ^d		50/50 ^e		20/80 ^f		80/20 ^g		50/50 ^h		80/20 ⁱ		50/50 ^j	
	$\log IE$	$\log IE^a$	α^b	$\log IE$	α	$\log IE$	α	$\log IE$	α	$\log IE$	α	$\log IE$	α	$\log IE$	α
tetrapropylammonium	4.97	4.97	1.00	4.83	1.00	4.38	1.00	4.98	1.00	4.77	1.00	5.03	1.00	4.92	1.00
tetraethylammonium	3.95	4.16	1.00	4.12	1.00	3.74	1.00	4.19	1.00	4.01	1.00	4.55	1.00	4.22	1.00
triethylamine	3.53	4.08	1.00	4.06	1.00	3.39	1.00	3.92	1.00	3.95	1.00	3.89	0.90	4.09	0.90
1-naphthylamine	4.04	3.92	0.95	3.82	0.95	3.40	0.95	3.47	0.08	2.51	0.08	3.20	0.00	3.54	0.00
N,N-dimethylaniline	3.72	3.75	1.00	3.71	1.00	3.37	1.00	2.38	0.56	2.36	0.56	0.91	0.00	1.94	0.00
diphenylphthalate	4.10	3.66	0.00	4.18	0.00		0.00	4.54	0.00	4.18	0.00	3.93	0.00	4.77	0.00
piperidine	3.16	3.47	1.00	3.40	1.00	2.91	1.00	3.33	1.00	2.90	1.00	3.23	0.96	3.32	0.96
pyrrolidine	2.70	3.20	1.00	2.53	1.00	2.33	1.00	2.54	1.00	2.38	1.00	2.31	0.97	2.93	0.97
dimethylphthalate	3.54	3.16	0.00	3.41	0.00	3.30	0.00	3.63	0.00	3.13	0.00	3.34	0.00	4.11	0.00
pyridine	2.94	3.13	1.00	2.44	1.00	2.41	1.00	1.77	0.67	1.43	0.67	-0.22	0.00	1.15	0.00
<i>consistency</i>															
<i>standard deviation</i>	0.30	0.16		0.18		0.02		0.13		0.15		0.21		0.18	
<i>two times combined</i>															
<i>standard deviation^l</i>		0.32		0.39		0.06		0.28		0.34		0.45		0.39	
pH ^k		2.68						5				9.75			

^a $\log IE$ values obtained via least-squares minimisation procedure (see 2.3) and anchored to tetrapropylammonium $\log IE$ value; ^b The approximate ionisation degree in solution (α) is calculated using the aqueous phase pH obtained by glass electrode and aqueous pK_a values; ^c $\log IE$ values in ref. [16]; ^d solvent system acetonitrile:0.1% formic acid 80:20 (v/v); ^e solvent system acetonitrile:0.1% formic acid 50:50 (v/v); ^f solvent system acetonitrile:0.1% formic acid 20:80 (v/v); ^g solvent system acetonitrile:pH=5.0 buffer 80:20 (v/v); ^h solvent system acetonitrile:pH=5.0 buffer 50:50 (v/v); ⁱ solvent system acetonitrile:1mM ammonia 80:20 (v/v); ^j solvent system acetonitrile:1mM ammonia 50:50 (v/v); ^k aqueous phase pH obtained with glass electrode; ^l combined standard deviation calculated using equation VII; ^m Diphenylphthalate could not be measured in solvent system due to poor solubility.

Table 2. The results of t-tests on the obtained ionisation efficiency scales in different solvent systems

	Compared solvents		Statistically significant difference in logIE value
pH change	Solvent 1	Solvent 4	1-naphthylamine, N,N-dimethylaniline, pyrrolidine, pyridine, diphenylphthalate
	Solvent 1	Solvent 6	tetraethylammonium, 1-naphthylamine, N,N-dimethylaniline, pyrrolidine, pyridine
	Solvent 2	Solvent 5	1-naphthylamine, N,N-dimethylaniline, piperidine, pyridine
	Solvent 2	Solvent 7	1-naphthylamine, N,N-dimethylaniline, pyrrolidine, pyridine, diphenylphthalate
	Solvent 4	Solvent 6	diphenylphthalate, N,N-dimethylaniline, pyridine
	Solvent 5	Solvent 7	N,N-dimethylaniline, diphenylphthalate, 1-naphthylamine, dimethylphthalate, piperidine, pyrrolidine
Change of organic phase percentage	Solvent 1	Solvent 2	diphenylphthalate, pyrrolidine, pyridine
	Solvent 1	Solvent 3	all except dimethylphthalate
	Solvent 2	Solvent 3	tetrapropylammonium, tetraethylammonium, triethylamine, 1-naphthylamine, piperidine
	Solvent 4	Solvent 5	diphenylphthalate, 1-naphthylamine, dimethylphthalate, piperidine, pyridine
	Solvent 6	Solvent 7	diphenylphthalate, dimethylphthalate, N,N-dimethylaniline, pyrrolidine, pyridine

The changes in logIE values with different water phase pH-s were for some analytes quite big and therefore additional 27 analytes were analysed in two solvent systems (acetonitrile/0.1% trifluoroacetic acid 80/20 and acetonitrile/pH=7 5 mM buffer 80/20). In Table 3 the results of water phase pH studies are presented. The pK_a value in water of studied analytes is in the range of studied water phase pH-s. The analytes were divided into two groups: pH independent and pH dependent analytes. pH independent means in this study that the logIE values obtained in two solvent systems (water phase pH=2.1 and 7) are not statistically significantly different (differ less than 0.5 logarithmic units).

Table 3. The results of water phase pH studies. pH independent analytes show $\log IE$ values with acetonitrile/0.1% trifluoroacetic acid (pH=2.11) 80/20 and with acetonitrile /pH=7.0 80/20 that do not differ statistically significantly. pH dependent analytes show $\log IE$ values that differ statistically significantly.

The pH independent analytes	pH dependent analytes
8-aminoquinaldine, 3(dimethylamino) benzoic acid, 2,6-diaminopyridine, 2,6(NO ₂) ₂ Ph-N=P1(pyrr) phosphazene , 3-hydroxypyridine, 4-amino-N,N-dimethylaniline, acridine, tris(hydroxymethyl)-aminomethane, 4(dimethylamino)-N,N-dimethylaniline, N,N-diphenylbispidine, 4-nitroaniline, 2-aminopyridine, 2-amino benzimidazole, 3-hydroxyaniline, 2,4,6-trinitroaniline	Pyridine, 2-aminophenol, 3-amino benzoic acid, aniline, 3-nitroaniline, 2-nitroaniline, 2,6-dimethylpyridine, quinoline, 3-methoxy-N,N-dimethylaniline, N,N-dimethylaniline, dimethylphenylphosphine, trimethylphosphine, 1-naphthylamine, 4-amino benzoic acid, 2,4-dinitroaniline

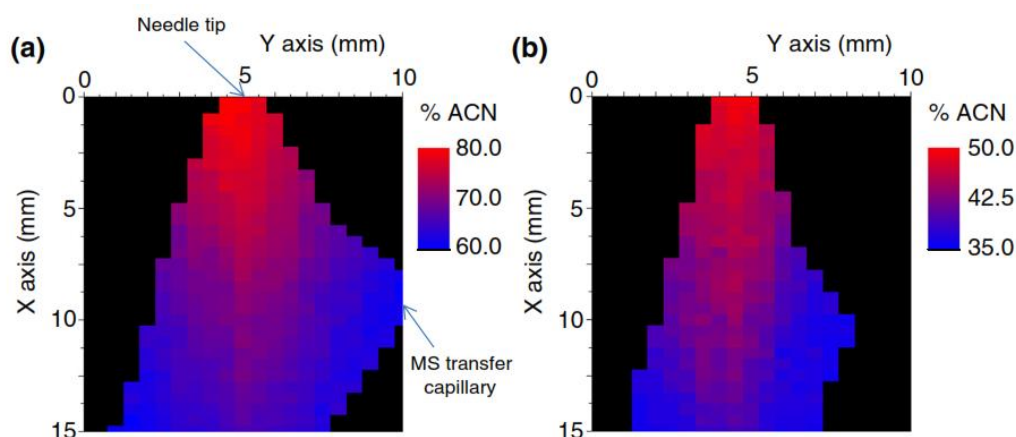


Figure 2. XY image of solvent fractionation in the plume (% of acetonitrile) from the fluorescence signal of 20 μM of Nile Red in A) solvent system (6), B) solvent system (7). Solvent flow rate 1 mL/h.

To study how the organic solvent content changes during electro spray the spray were recorded with fluorescence spectrometer. The evolution of the acetonitrile percentage in the electro spray plume, obtained by measuring the fluorescence signal of Nile Red, is presented in Figure 2. The measurement was carried out with one water phase of 1 mM ammonia, but one can assume that the fractionation does not depend significantly on water phase pH. It was observed that acetonitrile percentage decreases along the plume due to the observed solvent fractionating. In case of solvent system (6) the acetonitrile percentage decreases from 80% (needle tip, see

Figure 2: X; Y = 0; 5), which corresponds to the initial solvent fraction of the infused solution, to 61% (MS transfer capillary, X; Y = 8.8; 10). For solvent system (7), it was not possible to determine the acetonitrile percentage at the MS transfer capillary because not enough fluorescence signal was observed at this point. Indeed, the fluorescence of Nile Red in more than 65% water (in which it is only slightly soluble) is strongly quenched [47]. If the intersection of two solvent systems acetonitrile percentage evolution pictures are compared it is seen that by solvent system (6) the initial concentration of acetonitrile (80%) (X; Y = 0; 5.5) decreases to 63% (X; Y = 10; 8.5) and for solvent system (7) the acetonitrile percentage decreases from 50% to 36%.

To apply the ionisation efficiency approach in broad audience it is necessary to show that ionisation efficiency does not differ significantly on different mass spectrometric setups. The results of $\log IE$ measurements on different mass spectrometric setups are presented in Table 4. Altogether 102 relative measurements with 10 compounds were carried out during 1 month on every mass-spectrometer setup in 2 solvent systems. For each studied combination of MS setup and solvent system an ionisation efficiency scale was compiled. The compounds set covers 2.3 magnitudes of ionisation efficiency values. The ionisation efficiencies obtained with different mass spectrometers correlate quite well ($R^2 = 0.64-0.94$). The obtained $\log IE$ values for different instruments were also compared compound wise and the results are presented in Table 5. Although there were analytes that have statistically significantly different ionisation efficiencies on different mass spectrometric setups the order of ionisation efficiencies differed little.

Table 4. The positive mode ESI ionisation efficiency ($\log IE$) values in two solvent compositions on three different mass spectrometers with four different ESI setups.

	Acetonitrile /0.1% HCOOH						
	80/20				20/80		
	XCT ^a	Q ^b	3Q ^c	XCT-3R ^d	XCT	Q	3Q
tetrapropylammonium	4.83	5.17	4.63	4.57	4.38	4.22	3.80
tetraethylammonium	4.13	4.37	4.37	3.78	3.74	3.46	3.62
triethylamine	3.98	3.73	3.79	3.18	3.39	3.14	3.56
1-naphthylamine	3.84	3.67	3.92	3.31	3.40	3.22	3.04
N,N-dimethylaniline	3.68	3.41	4.01	3.22	3.37	2.97	2.92
diphenylphthalate	3.60	3.87	3.62	2.85	NA ^g	NA ^g	NA ^g
piperidine	3.38	3.61	3.70	2.62	2.91	3.00	3.15
pyrrolidine	3.16	3.61	3.56	2.80	2.33	3.01	2.97
dimethylphthalate	3.08	3.71	3.54	2.43	3.30	3.50	NA ^f
pyridine	2.97	3.19	3.47	2.36	2.41	2.71	2.87
<i>consistency standard deviation</i>	0.16	0.17	0.09	0.17	0.02	0.03	0.03
<i>two times combined standard deviation^e</i>	0.32	0.35	0.17	0.34	0.06	0.07	0.06
<i>Span</i>	1.87	1.98	1.16	2.21	2.05	1.51	0.93

^a Agilent XCT ion-trap with orthogonal ESI (see paragraph 2.2); ^b Agilent Single Quad 6100 with Agilent JetStream (see paragraph 2.2); ^c Varian J-320 (see paragraph 2.2); ^d Agilent XCT ion-trap with in house developed 3R sprayer (see paragraph 2.2); ^e combined standard deviation calculated using equation VII; ^f not measured ^g not possible to measure due to poor solubility;

Table 5. The results of bilateral comparison *t*-tests on the ionisation efficiency scales obtained on different mass spectrometers with different ESI setups and linear analysis results from scales comparison. Slope and intercept are obtained so that $\log IE$ values from I ESI setup are on x axis and $\log IE$ values from II setup are on y axis.

	I	II	Statistical differences	average difference	residuals standard deviation	Slope	Intercept	R ²
80/20	XCT	Q	tetrapropylammonium, dimethylphthalate, pyrrolidine	0.31	0.31	0.85±0.18	0.65±0.67	0.73
	XCT	3Q	tetrapropylammonium, tetraethylammonium, N,N-dimethylaniline, piperidine, dimethylphthalate, pyrrolidine, pyridine	0.28	0.15	0.63±0.09*	1.57±0.34*	0.86
	XCT	XCT-3R	all	0.28	0.18	1.15±0.11	-1.09±0.40*	0.94
	Q	3Q	tetrapropylammonium, N,N-dimethylaniline	0.23	0.22	0.58±0.13*	1.65±0.50*	0.71
	Q	XCT-3R	all except N,N-dimethylaniline	0.72	0.34	1.05±0.20	-0.91±0.80	0.77
	3Q	XCT-3R	all except tetrapropylammonium	0.75	0.18	1.70±0.16*	-3.43±0.61*	0.93
20/80	XCT	Q	all except piperidine	0.29	0.24	0.59±0.14*	1.32±0.44*	0.73
	XCT	3Q	all except tetraethylammonium and triethylamine	0.38	0.24	0.43±0.13*	1.85±0.43*	0.64
	Q	3Q	tetrapropylammonium, triethylamine	0.20	0.22	0.66±0.18	1.13±0.58	0.69

* slope value differs statistically significantly from 1 and intercept value differs statistically significantly from 0
Correlation curves between $\log IE$ values obtained for the different setups are shown in Appendix Figure S 8 to Figure S 16.

To prove the universality of ionisation efficiency scales a set of 15 compounds was studied on ICR mass spectrometric setup that was not included in the studied mass spectrometric setups. The compound set was studied in solvent system acetonitrile/0.1% formic acid 80/20 (v/v). The pH independent compounds – tetrahexylammonium, tetraethylammonium and tetramethylammonium – were chosen as calibrants. A correlation line between calibrants $\log IE$ values from ref. [16] and logarithm of sensitivity (signal to concentration ratio) was established. The obtained slope and intercept values together with corresponding $\log IE$ value from literature [16] were used to predict the concentration c_{calc} for each analyte. The results of independent validation are presented in Table 6. It can be observed that for none of the compounds obtained misprediction is larger than 2.5 times. Average difference was 1.39 times.

Table 6. The used concentrations (c_{sample}) and the predicted concentrations (c_{calc}) of independent validation

	$\log I/E$	c_{sample} (mol/L)	c_{calc} (mol/L)	$c_{\text{calc}}/c_{\text{sample}}$
tetramethylammonium	2.15	5.25E-06	NA ^b	
2-nitroaniline	2.44	2.36E-06	3.25E-06	0.73
benzamide	2.74	9.57E-07	1.42E-06	0.67
pyridine	2.94	4.89E-06	1.96E-06	2.49
piperidine	3.16	9.42E-07	4.92E-07	1.91
2,6-dimethylpyridine	3.41	3.50E-06	4.87E-06	0.72
triethylamine	3.53	6.66E-07	4.59E-07	1.45
N,N-dimethylaniline	3.72	1.02E-06	5.84E-07	1.74
tetraethylammonium	3.95	9.40E-07	NA ^b	
DBU (see Table S 1)	3.96	8.53E-07	1.57E-06	0.54
acridine	4.42	9.05E-07	7.95E-07	1.14
diphenylguanidine	4.61	4.08E-07	2.78E-07	1.46
tetrapropylammonium	4.97	3.82E-07	1.79E-07	2.14
tetrabutylammonium	5.13	2.83E-07	1.73E-07	1.63
tetrahexylammonium	5.65	7.96E-08	NA ^b	

^a values from ref. [16]

^b values used for calibration

4 Discussion

4.1 Mobile Phase Effects

4.1.1 Comparison with Earlier Results

In this study the ionisation efficiency scale was established using optimised ion optics parameters. Comparing the $\log IE$ values between this study and study by Oss et al. [16] with the t-test reveals that the differences are statistically insignificant. Therefore the previous study [16] remains valid even in the context of improved ion optics parameters implemented in this study. This shows on one hand that the previously established scale is sufficiently universal and on the other hand gives evidence that the scales established in this study are valid.

4.1.2 The Impact of Solvent pH

The number of ions generated from a substance at a given concentration depends not only on the compound but on the solvent system composition as well. Therefore the relative ionisation efficiency values vary between solvent systems.

It can be assumed that some of the compounds are charged already in the solvent and some become charged either in gas phase or on the superacidic media of the droplet surface. Unfortunately it is impossible to accurately calculate the degree of ionisation in the used solvents. Therefore in this work we assume that ionisation degrees calculated on the basis of water phase pH and pK_a values are a good approximation of ionisation occurring in the used mobile phase. A similar assumption has previously been used to be valid for anions in negative ion mode [21].

Based on the water phase pK_a values of the analytes (see Table 1) the compounds could be divided into three groups: analytes where $pK_a \gg$ solvent pH, $pK_a \ll$ pH and $pK_a \sim$ pH.

If the ionisation degrees in solution are calculated (see Table 1) and compared with $\log IE$ values some trends appear. In the case of analytes for which the ionisation degree in solution does not change markedly from solvent to solvent, either being 1 or approximately zero, ionisation efficiency does not depend significantly on the pH of the solvent system either. In the case of analytes with ionisation degree in solution varying significantly between solvent systems, the ionisation efficiencies varies as well. It is seen that there are three compounds for which the ionisation degree changes in the aqueous phases of the three solutions: pyridine, N,N-dimethylaniline and 1-naphthylamine. Comparing the $\log IE$ values of pyridine in these solvents: 3.13, 1.77 and -0.22 (80% acetonitrile and the corresponding aqueous phase composition: 0.1% formic acid (pH=2.68), pH 5.0 buffer, 1mM NH_3 (pH=9.75)) and the

corresponding ionisation degree in solutions: 1.00, 0.67 and 0.00, we can see that the lower the ionisation degree in solution, the lower the $\log IE$ value. Similar trends are seen for N,N-dimethylaniline and 1-naphthylamine. The change of $\log IE$ values in solvents with 80% organic phase and different aqueous phase compositions is statistically significant in the case of N,N-dimethylaniline, pyridine and occasionally 1-naphthylamine. On the other hand, the analytes with nearly zero ionisation degree can still give relatively good ionisation efficiency, as is seen in the example of diphenylphthalate and dimethylphthalate. Their ionisation degrees are nearly zero in all solvents but the $\log IE$ values in the used solvent systems are in the range of 4.77 to 3.66 for diphenylphthalate and 4.11 to 3.13 for dimethylphthalate. The possible reason is that although the concentration of protonated phthalate esters in the droplets is very small, they are ejected from the droplet very efficiently because they are (1) hydrophobic and (2) the chelated proton is poorly accessible for solvent molecules, hindering the efficient solvation of the ion. Another possibility is the existence of highly acidic (possibly superacidic) conditions in droplets, possibly caused by several H^+ ions in the droplet and insufficient number of solvent molecules to properly solvate them, leading to high activity of protons. Enami et al. [48] have shown that interfacial hydronium ion (on the ESI droplet surface) behaves as a superacid.

In order to study the solvent pH effect further, 30 analytes with $pK_a \sim$ water phase pH were studied in solvent systems with water phase pH values of 2.1 and 7. Therefore, for all of these compounds the ionisation degree changes for these mobile phases. It was observed that for some analytes $\log IE$ did change with pH and for some no change in $\log IE$ was observed (see Table 3). From this study it is clear that ionisation degree in liquid phase does not solely describe the ionisation efficiencies in different solvent systems. Comparing these two groups, the differences between the analytes are fuzzy. However one can conclude that larger and more hydrophobic analytes do not depend on water phase pH. Secondly it is evident that analytes with more than one basicity centre do not depend on water phase pH.

4.1.3 *The Impact of Organic Phase Percentage*

Comparing the ionisation efficiencies in different solvent systems it is seen that the ionisation efficiency somewhat depends on the organic phase percentage as well. The higher is the organic phase content in the solvent the higher is the ionisation efficiency (Table 1). The ionisation efficiency values were correlated with computational partition coefficients from ref. [16] and there is no significant correlation ($R^2 < 0.2$) between them. One of the reasons for the weak correlation can be that the solvent composition changes during the spray and we do not know the actual solvent composition at the exact moment when ionisation occurs (see Figure 2). It is

shown with fluorescence measurements that acetonitrile percentage decreases by at least 20 percent if the initial acetonitrile percentage is 80% and by at least 15 or slightly more percent in case of 50% initial acetonitrile percentage. Therefore the partition coefficients, calculated for initial solvent composition can be incompatible with the actual environment where gas phase ions are produced.

It is known that the ionisation efficiency is a joint property of the analyte and the solvent system. The organic phase percentage affects the droplet “drying” rate. Girod et al. [30] have shown that faster evaporation results in quicker decrease of droplet radius. Iribarne et al. [24] suggested that there is a crossing point in droplet radius when Coulomb fission is taken over by ion evaporation. Therefore when the droplet radius decreases quicker, the crossing point is achieved earlier and the ions have more time to evaporate resulting in higher ionisation efficiency. The solvent’s ability to support ionisation largely compensates for the low extent of protonation of the weakly basic compounds. If the acetonitrile percentage decreases from 80% to 50%, the $\log IE$ values decrease statistically significantly for pyrrolidine, pyridine and diphenylphthalate in case of 0.1% HCOOH water phase and for diphenylphthalate, 1-naphthylamine, dimethylphthalate, piperidine and pyridine in case of buffer pH=5.0 as water phase. In contradiction, in case of 1mM NH₃ water phase ionisation efficiency increase is observed for diphenylphthalate, dimethylphthalate, N,N-dimethylaniline, pyrrolidine and pyridine for decreasing acetonitrile content (from 80% to 50%).

In case of 50% organic phase the organic phase content decreases to 36% during ESI droplet evolution and therefore the analyte ions with lower hydrophobicity compared to neutral compounds are better solvated and evaporation into gas phase is suppressed.

Additionally, the organic phase percentage change can influence the droplet pH and the pK_a values of the bases and therefore affect the ionisation degree of bases. The increase of acetonitrile percentage to 60% decreases pK_a value of amines one unit [29]. This could be the reason why the $\log IE$ values of weak bases decrease with decreasing acetonitrile percentage.

Interestingly, it was observed that standard deviations obtained with solvent composition (3) are significantly smaller than with solvent composition (1) in the case of orthogonal pneumatically assisted ESI source and sheath gas assisted Jet Stream. In case of high acetonitrile percentage the solvent fractionation and drying rate are more affected by the drying and nebulising gas flow rate and temperature and the addition of a sheath gas due to the high volatility of acetonitrile. Electrospray plume obtained with a lower acetonitrile percentage

(20%) is less affected by the gas parameters due to the high proportion of less volatile water solvent. The solvent fractionation is less efficient whatever the gas parameters used which results in similar $\log IE$ values for the different systems.

4.2 Ionisation Efficiency Scale Universality

From the results in Table 4 it can be concluded that ionisation efficiency scales obtained in the same solvent system on different instruments have in broad terms similar IE orders. On all instruments tetrapropylammonium has the highest $\log IE$, followed by tetraethylammonium. Pyridine has the lowest IE on all instruments. In the middle of the scales there are differences and for some analytes they are statistically significant. On the other hand, correlation coefficients obtained while comparing data from different instruments range from acceptable to very good (R^2 0.64-0.94) (Table 5). Evaluating the obtained R^2 , the combined standard deviations (up to 0.35 $\log IE$ units) and spans (up to 2.21 $\log IE$ units) of the individual scales (See Table 4) the correlations are acceptable. Differences in the ionisation efficiency scales for the different setups could arise from the solution properties, the sprayer properties (i.e. source design) and the mass spectrometer properties (i.e. ion transport and detection).

4.2.1 Electrospray Source Design and Solution Properties

The scales could differ because of differences in electrospray sources. Indeed, the geometrical ESI source parameters that vary are the dimensions of the needle, the shape of needle tip, the geometry of electrospray setup (e.g. angle between needle and MS inlet capillary, on-axis or off-axis design) and the distance between needle tip and mass spectrometer inlet. Moreover, support gas parameters and voltages, such as the nebuliser gas pressure, drying gas temperature and flow rate, additional gas occurrence, the applied voltage between needle and mass spectrometer inlet and additional voltage occurrence, are different. These source properties are likely to cause differences in electrospray bloom – e.g. in solvent evaporation rate or droplet size variations. This can lead to differences in droplet compositions at which an average ion ejection occurs.

The results show that the ESI sprayer geometry is important. Comparing the spans with t -test there are statistically significant differences only between the scales obtained with the 3Q mass-spectrometer and other instruments (Table 5). The scales obtained with the 3Q mass-spectrometer are more than 1.5 times compressed compared to the ones obtained with the other MS systems. One reason could be that, in this ESI source, the needle is at approximately 120 degrees with respect to the mass spectrometer inlet capillary as opposed to the orthogonal geometry of the remaining ion sources. Compared to the orthogonal geometry of the remaining

ion sources the analytes have less time to evaporate from droplets and most of the droplets are blown to counter electrode [49]. Voyksner and Lee [50] and Holčápek et al. [51] have shown that orthogonal ESI source configuration gives better sensitivity than other source designs thanks to the prevention of clogging the MS orifice by non-volatile materials. Additionally, Tang and Smith [52] and Gomez and Tang [53] have shown that progeny droplets – sources for gas phase ions – are ejected in the sidewise direction toward the periphery region of the electrospray. Therefore, orthogonal source designs typically show better sensitivities.

Comparing the ionisation efficiencies obtained with the Jet Stream and with the orthogonal pneumatically assisted ESI source, the order of compounds in the scale changes. Additionally, regression analysis shows that the data points do not display as linear relationship as for other instruments. This could be explained by the fact that in the Jet Stream the optimum conditions are very analyte-dependent as shown by Stahnke et al. [54] and Periat et al. [49].

4.2.2 Mass Spectrometer Properties

In addition to source design, mass spectrometer may have an effect on ionisation efficiency. In this study we are unable to use the same ion source on different instruments and therefore it is not possible to statistically separate the effects of ion source and mass spectrometer. As also mentioned in the previous paragraph, the source geometry and the addition of drying gas affect the desolvation process in ESI. The early stages of ion train devices (i.e. transfer capillary, tube lens) may present different efficiencies with respect to partly desolvated ions.

4.3 Usefulness of Ionisation Efficiency Scales

The trends demonstrated by the IE scales obtained on different instruments are the same. Although the $\log IE$ values as a rule cannot be transferred from one MS setup to another, the scales give general information about ionisation efficiency: the statistical analysis of the obtained scales shows that they have differences but they correlate with each other. The order of compounds in the scale does not change remarkably and the ionisation efficiencies are consistent for the different setups, in the range of half logarithmic unit (equivalent to 3 times sensitivity difference). The good correlation between different scales also assures that models built for predicting ionisation efficiency are transferable between instruments and only the coefficients in the model may need some adjustment depending on the instrument.

It can be assumed that this type of adjustment can easily be carried out with measurements of three or more compounds from the scale on the new instrument. According to the obtained intensities, the adjustment of the predictive model can be made. Likely, three anchoring points

will be sufficient to scale the ionisation efficiencies and use them in semi-quantitative analysis as seen below (in paragraph 4.4).

For assessing the inter-instrument transferability of the ionisation efficiency scale, the ionisation efficiencies of three compounds - tetrapropylammonium, pyridine and N,N-dimethylaniline – obtained with the ion trap mass spectrometer and with another setup were correlated. The ion trap MS is chosen as reference point for this study because an extensive ionisation efficiency scale study for both positive [16] and negative [21] ionisation mode has been compiled with this instrument and the reliability of these scales has been demonstrated in a previous chapter (see paragraph 4.1.1). These three analytes were chosen to obtain an interpolative prediction model; tetrapropylammonium is the highest responder, pyridine is the lowest and N,N-dimethylaniline is situated in the middle of the scale measured on the ion trap instrument. In the predictive model the slopes and intercepts, if statistically significant, were used. The root mean square deviation of the differences between predicted ionisation efficiencies on different setups and the measured ionisation differences varied from 0.20 (triple quadrupole) to 0.36 (single quadrupole) $\log IE$ units. These are in the same range as the consistency standard deviations of obtained scales. Therefore, we have demonstrated that the built ionisation efficiency scale is transferable for different ESI/MS setups.

4.4 Independent Validation

The first preliminary models [7,16,21,42] for predicting ionisation efficiency are available, but each of them has been set up on a single instrument. In order to demonstrate the inter-instrument transferability the obtained $\log IE$ values from ref. [16] (orthogonal ESI source geometry and ion trap mass analyser) were applied to predict the concentrations of twelve analytes (7 of them were only used in validation set) on a completely different mass spectrometric setup (approximately 120 degree ESI source geometry and hybrid mass analyser that consist of triple quadrupole and FT-ICR). The used validation compounds set covers 3.5 $\log IE$ units. The data in Table 6 demonstrate that the concentrations of two compounds (pyridine and tetrapropylammonium) differ 2.0-2.5 times and for the remaining ten compounds the difference is less than 2 times. The average difference is 1.4 times. This validation gives additional support to the transferability of the $\log IE$ scale between different ESI/MS setups.

Conclusions

Although ESI/MS is a very widely used technique, there is still a lot unknown about processes happening in electrospray ionisation source. It is also unknown if mechanism of ionisation process is characteristic of the specific ESI source used or are completely universal. In order to know if ESI processes can be studied on one instrument and conclusions drawn also for other instruments it is important to study ionisation efficiencies on different instruments that have various ESI source geometries. Also current studies usually focus on one solvents. However, it has been noted that ionisation efficiencies depend significantly on the solvent used. Therefore it would be beneficial to know how exactly solvent affects the ionisation efficiencies.

In this master's thesis ionisation efficiency scale approach was used to study mobile phase effects on ionisation efficiency and transferability of ionisation efficiency scales between different mass spectrometric setups.

Following conclusions were made:

- higher organic phase content results in higher ionisation efficiency,
- the strong bases give high ionisation efficiency even in basic medium,
- very weak bases with high hydrophobicity can still give high ionisation efficiency,
- the analytes with pK_a value significantly higher than solvent pH or pK_a value significantly lower than solvent pH are independent on solvent pH,
- some of the analytes with pK_a in the range of solvent pH are influenced by solvent pH,
- ionisation efficiency scales obtained on different instruments are in good correlation to each other, and
- the ionisation efficiency scale is transferable between different mass spectrometric setups via three points linear calibration.

Therefore it was proven that ionisation efficiency trends are independent of mass spectrometric setup. Additionally, it was shown that mobile phase can change ionisation efficiency remarkably and therefore the effects of mobile phase should be included into model describing ESI process. These results give valuable input for developing standard substance free quantification model.

In order to fulfil this long term goal pH effect on ionisation efficiency should be studied in more detail and the ionisation efficiency relationship to effects of mobile phase should be described quantitatively.

References

1. Cole, R. B. *Electrospray and MALDI Mass Spectrometry Fundamentals, Instrumentation, Practicalities, and Biological Applications*; John Wiley & Sons: New Jersey, 2010.
2. Cech, N. B.; Enke, C. G. Practical Implications of Some Recent Studies in Electrospray Ionization Fundamentals. *Mass Spectrom. Reviews* **2001**, 362-387.
3. Yamashita, M.; Fenn, J. B. Electrospray Ion Source. Another Variation on the Free-Jet Theme. *J. Phys. Chem.* **1984**, 88, 4451-4459.
4. Yamashita, M.; Fenn, J. B. Negative Ion Production with the Electrospray Ion Source. *J. Phys. Chem.* **1984**, 88, 4671-4675.
5. Fenn, J. B. Nobel Lecture: Electrospray Wings for Molecular Elephants, 2002. http://www.nobelprize.org/nobel_prizes/chemistry/laureates/2002/fenn-lecture.html (accessed October 4, 2014).
6. Kebarle, P.; Tang, L. From Ions in Solution to Ions in the Gas Phase. The Mechanism of Electrospray Mass Spectrometry. *Anal. Chem.* **1993**, 65 (22), 972-986.
7. Chalcraft, K. R.; Lee, R.; Mills, C.; Britz-McKibbin, P. Virtual Quantification of Metabolites by Capillary Electrophoresis-Electrospray Ionization-Mass Spectrometry: Predicting Ionization Efficiency Without Chemical Standards. *Anal. Chem.* **2009**, 81, 2506-2515.
8. Ehrmann, B.; Henriksen, T.; Cech, N. B. Relative Importance of Basicity in the Gas Phase and in Solution for Determining Selectivity in Electrospray Ionization Mass Spectrometry. *J. Am. Soc. Mass Spectrom.* **2008**, 19, 719-7728.
9. Konermann, L.; Ahadi, E.; Rodriguez, A. D.; Vahidi, S. Unraveling the Mechanism of Electrospray Ionization. *Anal. Chem.* **2013**, 85, 2-9.
10. Liigand, J.; Kruve, A.; Leito, I.; Girod, M.; Antoine, R. Effect on Mobile Phase on Electrospray Ionization Efficiency. *J. Am. Soc. Mass Spectrom.* **2014**, 25, 1853-1861.
11. Tang, L.; Kebarle, P. Dependence of Ion Intensity in Electrospray Mass Spectrometry on the Concentration of the Analytes in the Electrosprayed Solution. *Anal. Chem.* **1993**, 65, 3654-3668.
12. Cech, N. B.; Enke, C. G. Relating Electrospray Ionization Response to Nonpolar Character of Small Peptides. *Anal. Chem.* **2000**, 72, 2717-2723.
13. Cech, N. B.; Krone, J. P.; Enke, C. G. Predicting Electrospray Response from Chromatographic Retention Time. *Anal. Chem.* **2001**, 73, 208-213.
14. Leito, I.; Herodes, K.; Huopola, M.; Virro, K.; Künnapas, A.; Kruve, A.; Tanner, R. Towards the electrospray ionization mass spectrometry ionization efficiency scale of organic compounds. *Rapid Commun. Mass Spectrom.* **2008**, 22, 379-384.

15. Henriksen, T.; Juhler, R. K.; Svensmark, B.; Cech, N. B. The Relative Influences of Acidity and Polarity on Responsiveness of Small Organic Molecules to Analysis with Negative Ion Electrospray Ionization Mass Spectrometry (ESI-MS). *J. Am. Mass. Spectrom.* **2005**, *16*, 446 – 455.
16. Oss, M.; Krueve, A.; Herodes, K.; Leito, I. Electrospray Ionization Efficiency Scale of Organic Compounds. *Anal. Chem.* **2010**, *82*, 2865–2872.
17. Yang, X. Y.; Qu, Y.; Yuan, Q.; Wan, P.; Du, Z.; Chen, D.; Wong, C. Effect of ammonium on liquid- and gas-phase protonation and deprotonation in electrospray ionization mass spectrometry. *Analyst* **2012**, *138*, 659 – 665.
18. Huffman, B. A.; Poltash, M. L.; Hughey, C. A. Effect of Polar Protic and Polar Aprotic Solvents on Negative-Ion Electrospray Ionization and Chromatographic Separation of Small Acidic Molecules. *Anal. Chem.* **2012**, *84*, 9942– 9950.
19. Amad, M. H.; Cech, N. B.; Jackson, G. S.; Enke, C. G. Importance of gas-phase proton affinities in determining the electrospray ionization response for analytes and solvents. *J. Mass. Spectrom.* **2000**, *35*, 784 –7789.
20. Krueve, A.; Kaupmees, K.; Liigand, J.; Oss, M.; Leito, I. Sodium adduct formation efficiency in ESI source. *J. Mass. Spectrom.* **2013**, *48* (6), 695-702.
21. Krueve, A.; Kaupmees, K.; Liigand, J.; Leito, I. Negative Electrospray Ionization via Deprotonation: Predicting the Ionization Efficiency. *Anal. Chem.* **2014**, *86*, 4822-4830.
22. Constantopoulos, T. L.; Jackson, G. S.; Enke, C. G. Effects of Salt Concentration on Analyte Response Using Electrospray Ionization Mass Spectrometry. *J. Am. Soc. Mass Spectrom.* **1999**, *10*, 625-634.
23. Dole, M.; Mack, L. L.; Hines, R. L.; Mobley, R. C.; Ferguson, L. D.; Alice, M. B. Molecular Beams of Macroions. *J. Chem. Phys.* **1968**, *49*, 2240-2249.
24. Iribarne, J. V.; Thomson, B. A. On the evaporation of small ions from charged droplets. *J. Chem. Phys.* **1976**, *64* (6), 2287-2294.
25. van Berkel, G. J.; McLuckey, S. A.; Glish, G. L. Electrochemical Origin of Radical Cations Observed in Electrospray Ionization Mass Spectra. *Anal. Chem.* **1992**, *64*, 1586-1593.
26. Kebarle, P.; Peschke, M. On the mechanisms by which the charged droplets produced by electrospray lead to gas phase ions. *Anal. Chim. Acta* **2000**, *406*, 11-35.
27. Kostianen, R.; Kauppila, T. J. Effect of eluent on the ionization process in liquid chromatography-mass spectrometry. *J. Chromatogr. A* **2009**, *1216*, 685-699.
28. Cole, R. B.; Harrata, A. K. Solvent effect on analyte charge state, signal intensity, and stability in negative ion electrospray mass spectrometry; implications for the mechanism of negative ion formation. *J. Am. Soc. Mass Spectrom.* **1993**, *4*, 546-556.

29. Subirats, X.; Roses, M.; Bosch, E. On the Effect of Organic Solvent Composition on the pH of Buffered HPLC Mobile Phase and the pKa of Analytes - A Review. *Sep. Pur. Rev.* **2007**, *36*, 231-255.
30. Girod, M.; Dagany, X.; Boutou, V.; Broyer, M.; Antoine, R.; Dugourd, P.; Mordehai, A.; Love, C.; Werlich, M.; Fjeldsted, J.; Stafford, G. Profiling an electrospray plume by laser-induced fluorescence and Fraunhofer diffraction combined to mass spectrometry: influence of size and composition of droplets on charge-state distributions of electrosprayed proteins. *Phys. Chem. Chem. Phys.* **2012**, *14*, 9389–9396.
31. Kostiane, R.; Bruins, A. P. Effect of Solvent on Dynamic Range and Sensitivity in Pneumatically-assisted Electrospray (Ion Spray) Mass Spectrometry. *Rapid Commun. Mass Spectrom.* **1996**, *10*, 1393-1399.
32. Ahadi, E.; Konermann, L. Ejection of Solvated Ions from Electrosprayed Methanol/Water nanodroplets Studied by Molecular Dynamics Simulations. *J. Am. Chem. Soc.* **2011**, *133*, 9354-9363.
33. Zhou, S.; Hamburger, M. Effects of Solvent Composition on Molecular Ion Response in Electrospray Mass Spectrometry: Investigation of the Ionization Processes. *Rapid Commun. Mass Spectrom.* **1995**, *9*, 1516-1521.
34. Ahadi, E.; Konermann, L. Surface Charge of Electrosprayed Water Nanodroplets: A Molecular Dynamics Study. *J. Am. Chem. Soc.* **2010**, *132*, 11270-11277.
35. Ahadi, E.; Konermann, L. Molecular Dynamics Simulations of Electrosprayed Water Nanodroplets: Internal Potential Gradients, Location of Excess Charge Centers, and "Hopping" Protons. *J. Phys. Chem.* **2009**, *113*, 7071-7080.
36. Mallet, C. R.; Lu, Z.; Mazzeo, J. R. A study of ion suppression effects in electrospray ionization from mobile phase additives and solid-phase extracts. *Rapid. Commun. Mass Spectrom.* **2004**, *18*, 49-58.
37. Zhou, S.; Cook, K. D. Protonation in Electrospray Mass Spectrometry: Wrong-Way-Round or Right-Way-Round? *J. Am. Soc. Mass Spectrom.* **2000**, *11*, 961-966.
38. Girod, M.; Dagancy, X.; Antoine, R.; Dugourd, P. Relation between charge state distributions of peptide anions and pH changes in the electrospray plume. A mass spectrometry and optical spectroscopy investigations. *Int. J. Mass Spectrom.* **2011**, *308*, 41-48.
39. van Berkel, G. J.; Zhou, F.; Aronson, J. T. Changes in bulk solution pH caused by the inherent controlled-current electrolytic process of an electrospray ion source. *Int. J. Mass Spectrom. Ion Proc.* **1997**, *162*, 55-67.
40. Subirats, X.; Bosch, E.; Roses, M. Retention of ionisable compounds on high-performance liquid chromatography: XV. Estimation of the pH variation of aqueous buffers with the change of the acetonitrile fraction of the mobile phase. *J. Chromatogr. A* **2004**, *1059*, 33-42.

41. Nguyen, T. B.; Nizkorodov, S. A.; Laskin, A.; Laskin, J. An approach toward quantification of organic compounds in complex environmental samples using high-resolution electrospray ionization mass spectrometry. *Anal. Methods* **2013**, *5*, 72 – 80.
42. Wu, L.; Wu, Y.; Shen, H.; Gong, P.; Cao, L.; Wang, G.; Hao, H. Quantitative structure-ion intensity relationship strategy to the prediction of absolute levels without authentic standards. *Anal. Chim. Acta* **2013**, *794*, 67-75.
43. Rodima, T.; Kaljurand, I.; Pihl, I.; Mäemets, V.; Leito, I.; Koppel, I. A. Acid-base equilibria in nonpolar media. 2. Self-consistent basicity scale in THF solution ranging from 2-methoxy-pyridine to EtP1(pyrr) phosphazene. *J Org Chem* **2002**, *67*, 1873-1881.
44. Toom, L.; Kütt, A.; Kaljurand, I.; Leito, I.; Ottosson, H.; Grennberg, H.; Gogoll, A. Substituent effects on the basicity on 3,7-diazabicyclo[3.3.1]nonanes. *J. Org. Chem.* **2006**, *71*, 7155-7164.
45. Kruve, A.; Leito, I.; Herodes, K.; Laaniste, A.; Lõhmus, R. Enhanced Nebulization Efficiency of Electrospray Mass Spectrometry: Improved Sensitivity and Detection Limit. *J. Am. Soc. Mass Spectrom.* **2012**, *23*, 2051-2054.
46. Kaljurand, I.; Kütt, A.; Sooväli, L.; Rodima, T.; Mäemets, V.; Leito, I.; Koppel, I. A. Extension of the self-consistent spectrophotometric basicity scale in acetonitrile to a full span of a 28 pK(a) units: Unification of different basicity scales. *J. Org. Chem.* **2005**, *70* (3), 1019-1028.
47. Greenspan, P.; Fowler, S. D. Spectrofluorometric studies of the lipid probe, Nile red. *J. Lipid Res.* **1985**, *26*, 781-789.
48. Enami, S.; Stewart, L. A.; Hoffmann, M. R.; Colussi, A. J. Superacid Chemistry on Mildly Acidic Water. *J. Phys. Chem. Lett.* **2010**, *1*, 3488-3493.
49. Periat, A.; Kohler, I.; Bugey, A.; Bieri, S.; Versace, F.; C., S.; Guilleme, D. Hydrophilic interaction chromatography versus reversed phase liquid chromatography coupled to mass spectrometry: Effect of electrospray ionization source geometry on sensitivity. *J. Chromatogr. A* **2014**, *1356*, 211-220.
50. Voyksner, R. D.; Lee, H. Improvements in LC/Electrospray Ion Trap Mass Spectrometry Performance Using an Off-Axis Nebulizer. *Anal. Chem.* **1999**, *71*, 1441-1447.
51. Holcapek, M.; Volna, K.; J. P.; Kolarova, L.; Lemr, K.; Exner, M.; Cirkva, A. Effects of ion-pairing reagents on the electrospray signal suppression of sulphonated dyes and intermediates. *J. Mass Spectrom.* **2004**, *39*, 43-50.
52. Tang, K.; D., S. R. Theoretical prediction of charged droplet evaporation and fission in electrospray ionization. *Int. J. Mass Spectrom.* **1999**, *187*, 97-105.
53. Gomez, A.; Tang, K. Charge and Fission of Droplets in Electrostatic Sprays. *Phys. Fluids* **1994**, *6*, 404-414.

54. Stahnke, H.; Kittlaus, S.; Kempe, G.; Hemmerling, C.; Alder, L. The influence of electrospray ion source design on matrix effects. *J. Mass. Spectrom.* **2012**, *47*, 875-884.
55. Varian, I. *300 Series LC/MS and GC/MS Quadrupole Mass Spectrometer Hardware Operation Manual*; Walnut Creek, 2008.

MOBIILSE FAASI EFEKTID IONISATSIOONIEFEKTIIVSUSELE JA IONISATSIOONIEFEKTIIVSUSTE SKAALADE ÜLEKANTAVUS ERINEVATELE MASSISPEKTROMEETRITELE.

Jaanus Liigand

Kokkuvõte

Vedelikkromatograafia massispektromeetria on laialdaselt rakendatud analüüsimeetod. Tänu ühendite lahutamise ning identifitseerimise võimalusele on see meetod väga väärtuslik nii keskkonna kui ka ravimianalüüsidel, aga ka fundamentaaluuringutes. Kuigi elektropihustusionisatsiooni liides on kommersiaalselt kättesaadav juba eelmise sajandi 90ndate algusest, on selle mehhanism lõpuni arusaamata.

ESI allikas annavad erinevad analüüdid sama kontsentratsiooni juures erineval määral gaasifaasilisi ioone st omavad erinevat ionisatsiooniefektiivsust. Seepärast on kvantiseerimiseks vajalik kalibreerimisgraafiku meetodi kasutamine. Mitmetes rakendustes on aga standardained raskesti kättesaadavad või puuduvad hoopis. Sellise probleemi parem lahendus oleks rakendada analüüdi ionisatsiooniefektiivsuse ennustumudelit, mis võimaldaks standardaine vaba kvantiseerimist.

Kuigi analüüdi ionisatsiooniefektiivsuse sõltuvust analüüdi füsikokeemilistest parameetritest on uuritud, puudub kvantitatiivne uuring ionisatsiooniefektiivsuse solventiefektide kohta.

Selle magistritöö eesmärgiks oli uurida mobiilfaasi koostise mõju ainete ionisatsiooniefektiivsustele. Nende mõjude uurimiseks rakendati ionisatsiooniefektiivsuste skaala meetodit, mis võimaldab efekte kvantitatiivselt hinnata. Samuti pakkus huvi, kas ühe massispektrometri peal leitud ionisatsiooniefektiivsused on ülekantavad ka teistele instrumentidele. Seetõttu võrreldi omavahel nelja erineva ioonallika ja kolme erineva massianalüsaatoriga massispektromeetreid.

Käesolevas töös leiti, et ühendite ionisatsiooniefektiivsust mõjutavad nii orgaanilise solventi sisaldus kui ka veefaasi pH. Kõrgem orgaanilise solventi sisaldus parendab analüütide ionisatsiooniefektiivsust. Solventi pH mõjutab ühendeid, mille pK_a on solventi pH lähedane. Seevastu tugevad alused ioniseeruvad hästi isegi aluselises keskkonnas. Samas ka väga nõrgad, kuid väga hüdrofoobsed alused on kõrge ionisatsiooniefektiivsusega.

Lisaks sellele näidati, et ionisatsiooniefektiivsuste skaala trendid on universaalsed erinevate instrumentide üleselt. Käesolevas töös näidati, et ionisatsiooniefektiivsuste skaalad on erinevate seadmete vahel kolme punkti kalibratsiooniga üle kantavad.

Acknowledgements

This study was supported by national scholarship program Kristjan Jaak, which is funded and managed by Archimedes Foundation in collaboration with the Ministry of Education and Research. I thank Tõiv Haljasorg for instrumental assistant. I thank Dr. Marion Girod and Dr. Rodolphe Antoine, his research group and University of Lyon 1 for possibility to image the ESI plume.

Appendix

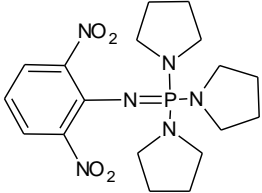
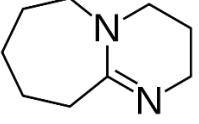
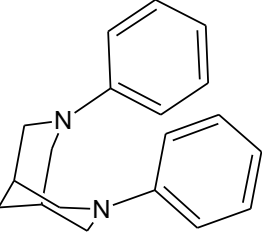
Name	Structure
2,6-(NO ₂) ₂ -C ₆ H ₃ -P1(pyrr) phosphazene	
DBU	
N,N-diphenylbispidine	

Table S 1. Structure of compounds

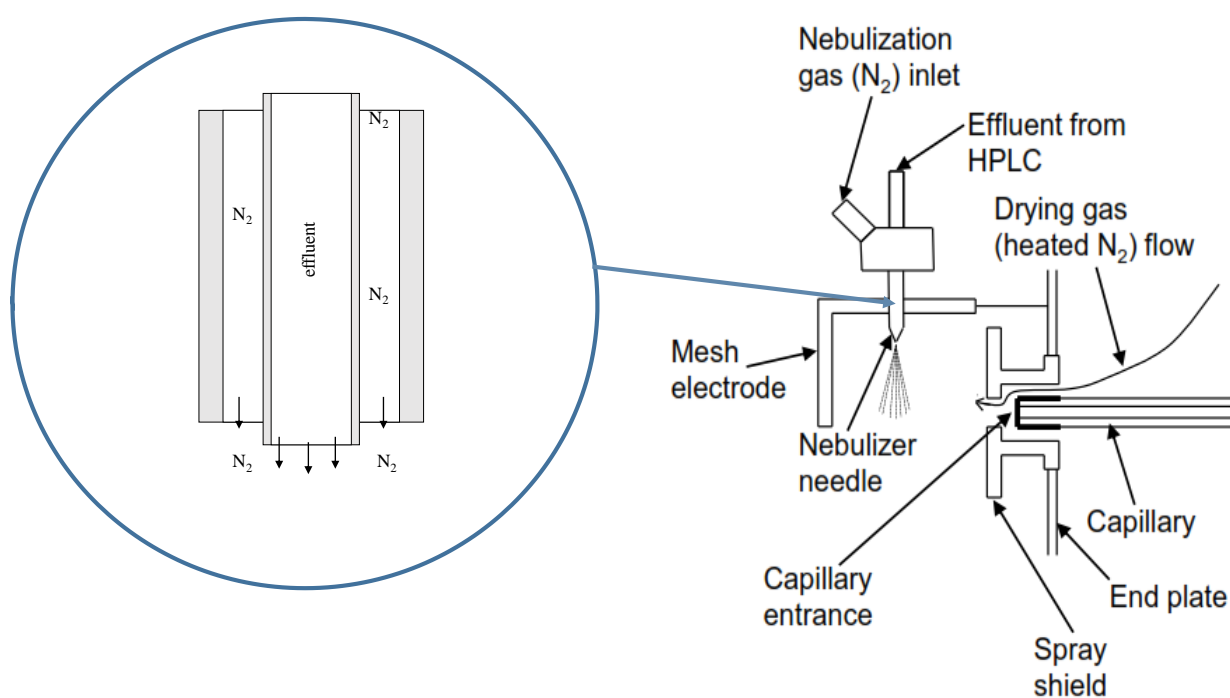


Figure S 1. Agilent conventional pneumatically assisted ESI source.

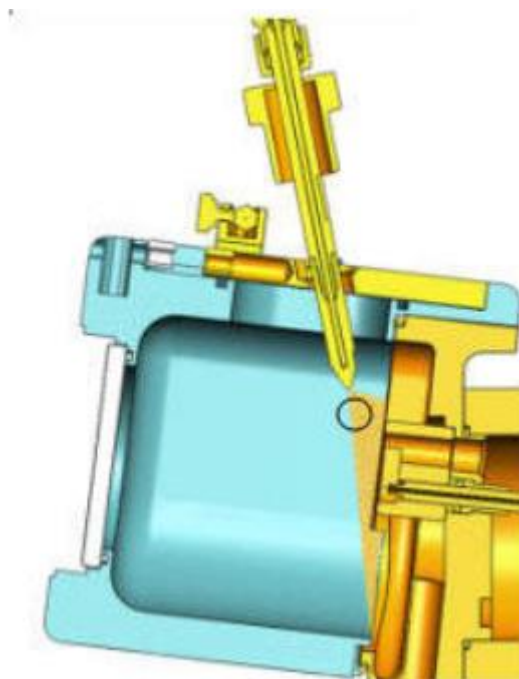


Figure S 2. ESI source in case of Varian J-320 triple quadrupole mass spectrometer [55].

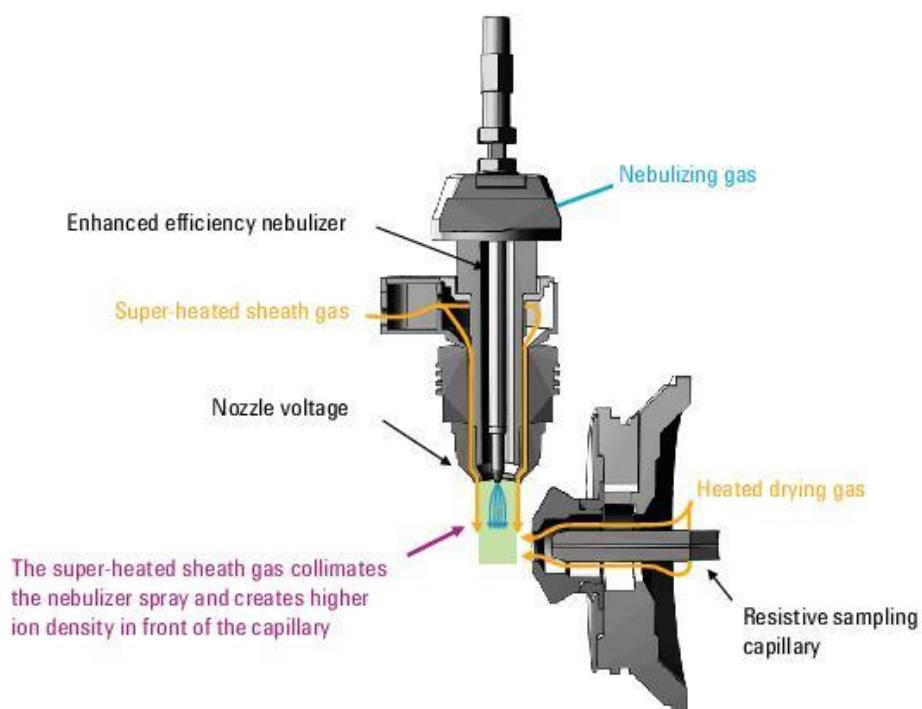


Figure S 3. Agilent Jetstream ESI source (figure obtained from Agilent Technologies).

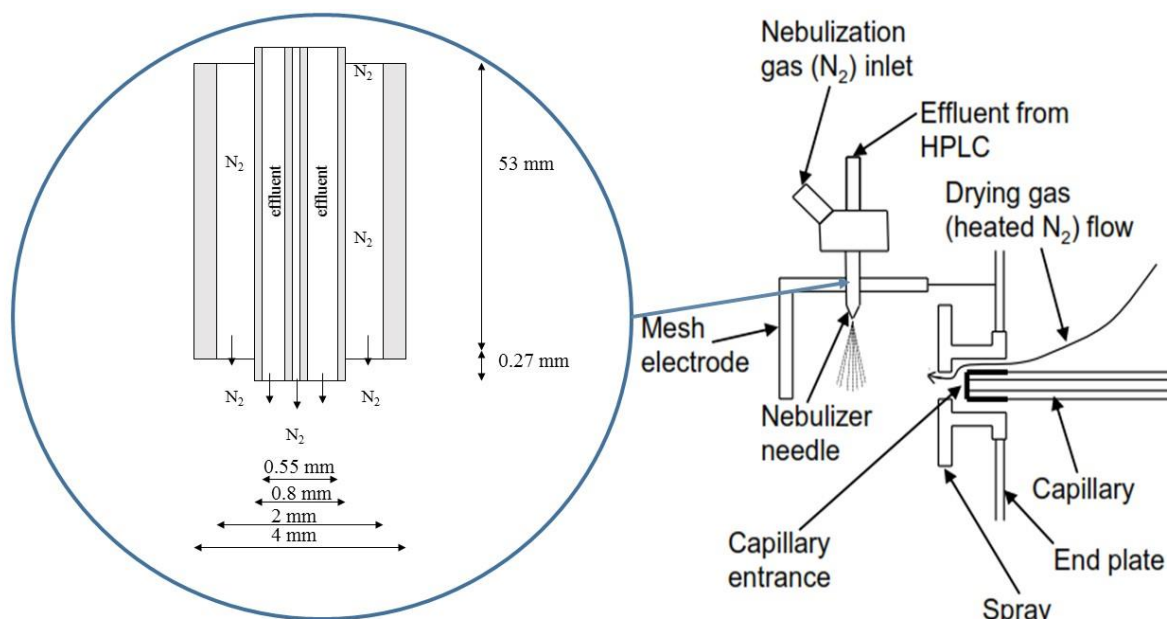


Figure S 4. in-house developed 3-R sprayer [45].

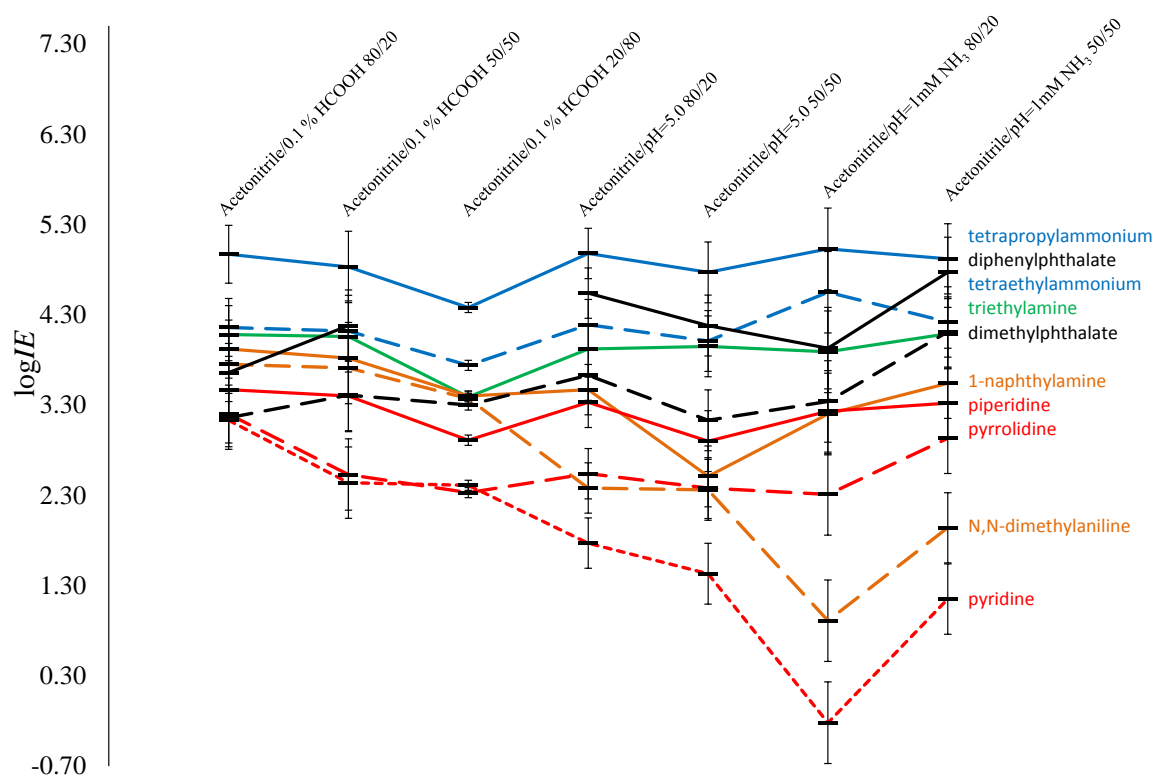


Figure S 5. The positive ion mode ESI ionisation efficiency ($\log IE$) values in different solvent compositions. Error bars correspond to $2 \sigma_c$ (Eq. VII)

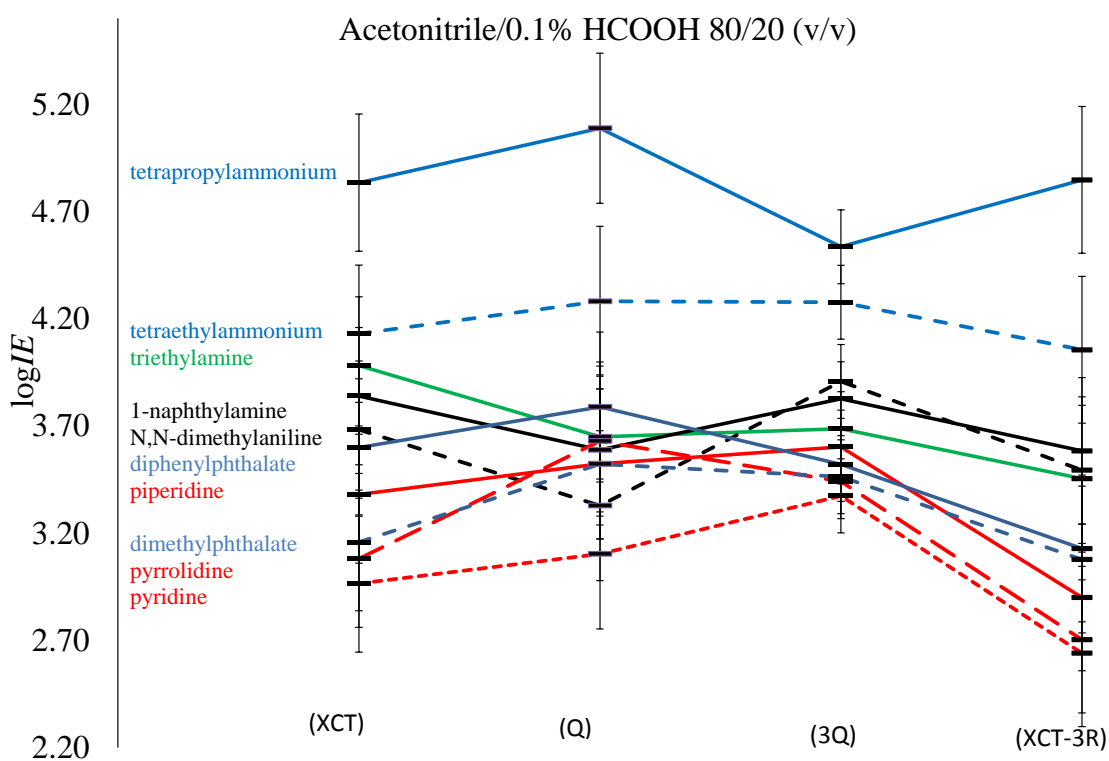


Figure S 6. The ESI positive mode ionisation efficiency ($\log IE$) values in on different mass spectrometer in acetonitrile/0.1% HCOOH in pure-water 80/20 (v/v) solvent mixture. The abbreviations on bottom of diagram show the corresponding mass spectrometer (see paragraph 2.2). Error bars correspond to double combine standard deviation.

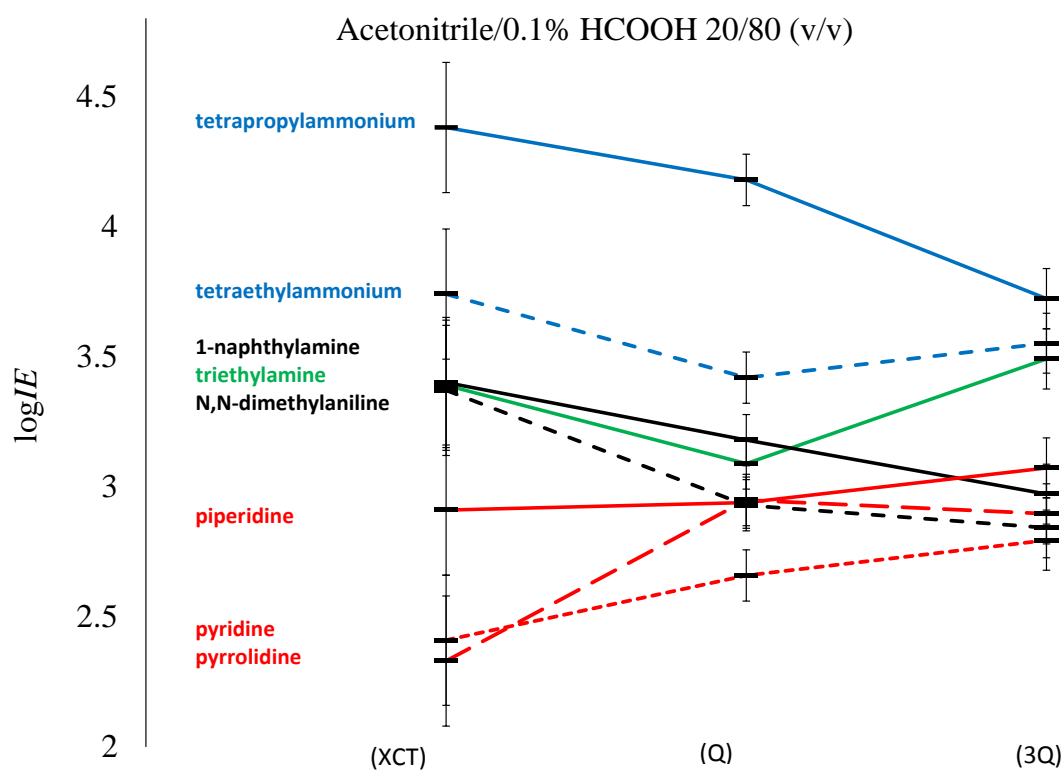


Figure S 7. The ESI positive mode ionisation efficiency ($\log IE$) values in on different mass spectrometer in acetonitrile/0.1% HCOOH in pure-water 20/80 (v/v) solvent mixture. The abbreviations on bottom of diagram show the corresponding mass spectrometer (see paragraph 2.2). Error bars correspond to double combine standard deviation.

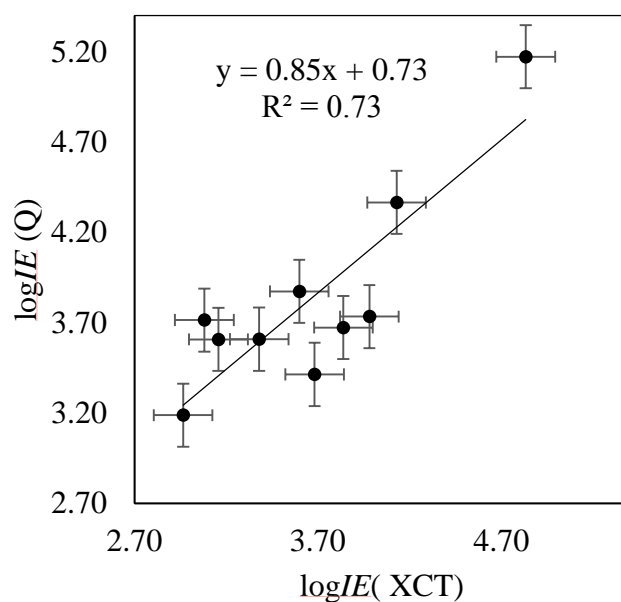


Figure S 8. Correlation curve between $\log IE$ values obtained with Agilent XCT IonTrap (x-axis) and Agilent Single Quad (y-axis) in case of acetonitrile/0.1% HCOOH 80/20 (v/v) solvent composition.

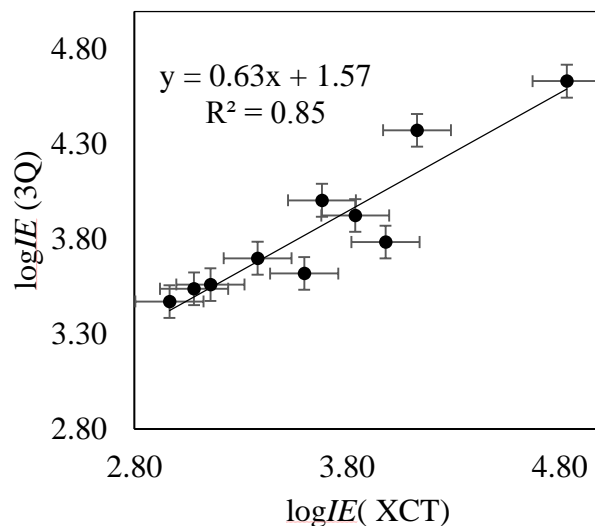


Figure S 9. Correlation curve between $\log IE$ values obtained with Agilent XCT IonTrap (x-axis) and Varian J-320 (y-axis) in case of acetonitrile/0.1% HCOOH 80/20 (v/v) solvent composition.

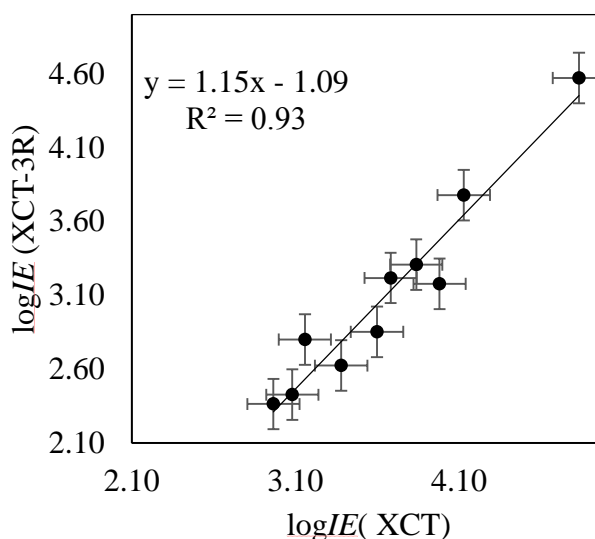


Figure S 10. Correlation curve between $\log IE$ values obtained with Agilent XCT IonTrap (x-axis) and Agilent XCT Iontrap equipped with in-house developed ESI source (y-axis) in case of acetonitrile/0.1% HCOOH 80/20 (v/v) solvent composition.

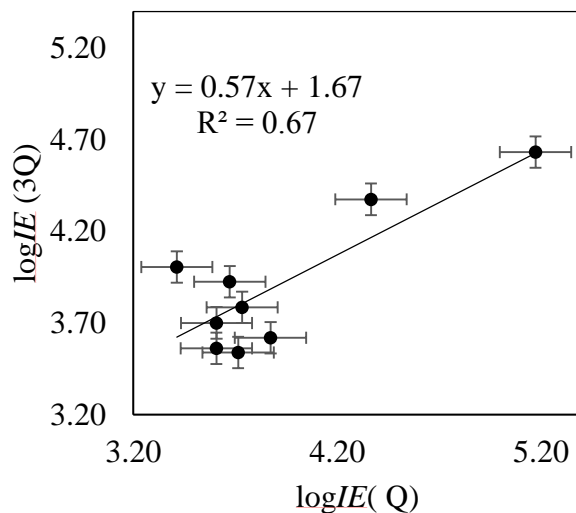


Figure S 11. Correlation curve between $\log IE$ values obtained with Agilent Single Quad (x-axis) and Varian J-320 (y-axis) in case of acetonitrile/0.1% HCOOH 80/20 (v/v) solvent composition.

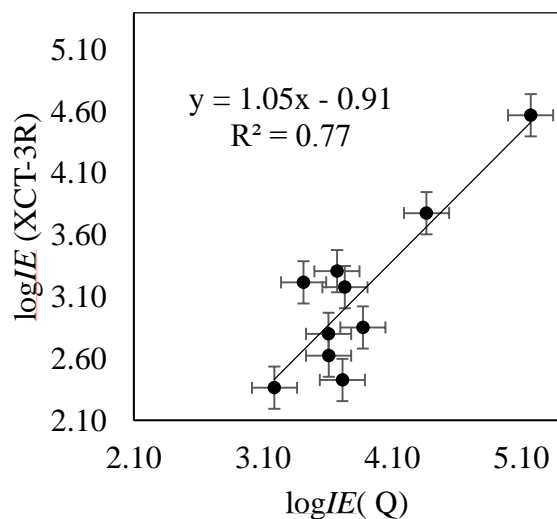


Figure S 12. Correlation curve between $\log IE$ values obtained with Agilent Single Quad (x-axis) and Agilent XCT Iontrap equipped with in-house developed ESI source (y-axis) in case of acetonitrile/0.1% HCOOH 80/20 (v/v) solvent composition.

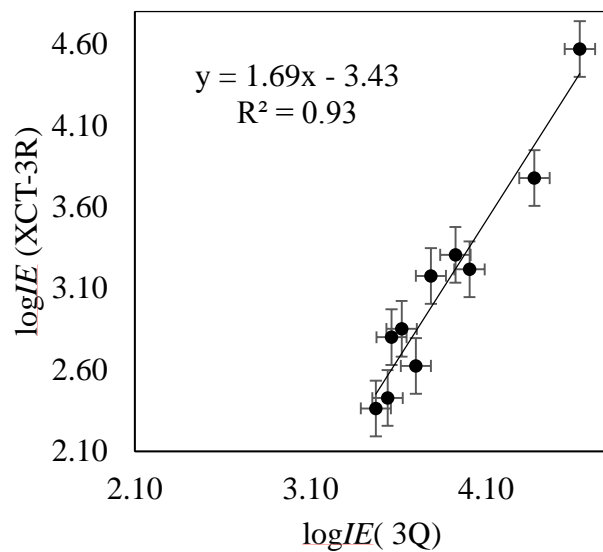


Figure S 13. Correlation curve between $\log IE$ values obtained with Varian J-320 (x-axis) and Agilent XCT Iontrap equipped with in-house developed ESI source (y-axis) in case of acetonitrile/0.1% HCOOH 80/20 (v/v) solvent composition.

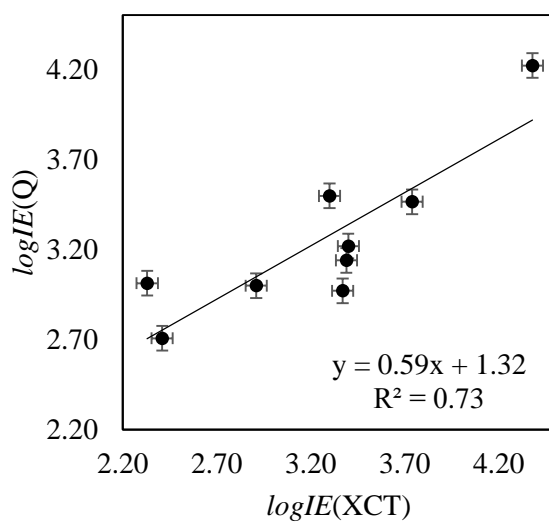


Figure S 14. Correlation curve between $\log IE$ values obtained with Agilent XCT IonTrap (x-axis) and Agilent Single Quad (y-axis) in case of acetonitrile/0.1% HCOOH 20/80 (v/v) solvent composition.

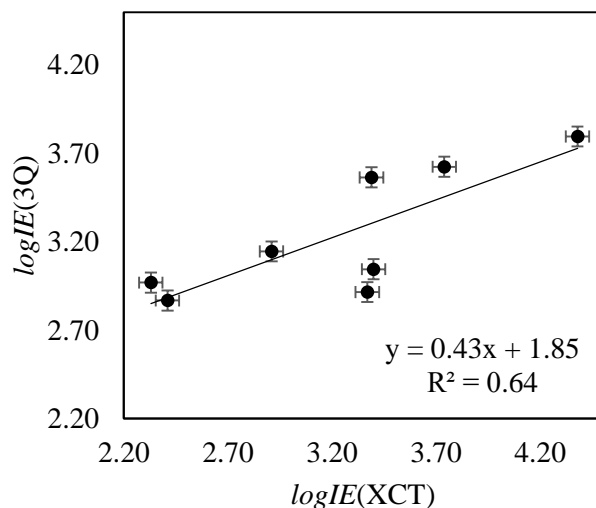


Figure S 15. Correlation curve between $\log IE$ values obtained with Agilent XCT IonTrap (x-axis) and Varian J-320 (y-axis) in case of acetonitrile/0.1% HCOOH 20/80 (v/v) solvent composition.

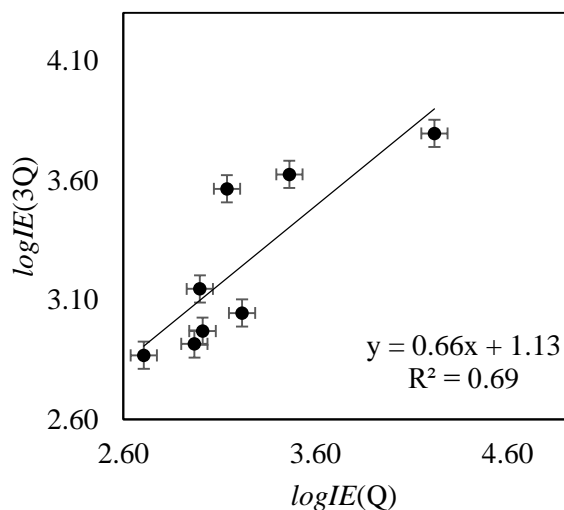


Figure S 16. Correlation curve between $\log IE$ values obtained with Agilent Single Quad (x-axis) and Varian J-320 (y-axis) in case of 20/80 (v/v) solvent composition.

Lihtlitsents lõputöö reprodutseerimiseks ja lõputöö üldsusele kättesaadavaks tegemiseks

Mina, _____ Jaanus Liigand _____,

(autori nimi)

annan Tartu Ülikoolile tasuta loa (lihtlitsentsi) enda loodud teose

**ELECTROSPRAY IONISATION EFFICIENCY SCALES:
MOBILE PHASE EFFECTS AND TRANSFERABILITY**

(lõputöö pealkiri)

mille juhendaja on _____ dr. Anneli Kruve _____,

(juhendaja nimi)

reprodutseerimiseks säilitamise ja üldsusele kättesaadavaks tegemise eesmärgil, sealhulgas digitaalarhiivi DSpace-is lisamise eesmärgil kuni autoriõiguse kehtivuse tähtaja lõppemiseni;

üldsusele kättesaadavaks tegemiseks Tartu Ülikooli veebikeskkonna kaudu, sealhulgas digitaalarhiivi DSpace'i kaudu alates 02.06.2018 kuni autoriõiguse kehtivuse tähtaja lõppemiseni.

olen teadlik, et nimetatud õigused jäävad alles ka autorile.

kinnitan, et lihtlitsentsi andmisega ei rikuta teiste isikute intellektuaalomandi ega isikuandmete kaitse seadusest tulenevaid õigusi.

Tartus 25.05.2015